MicroRNA-138-1-3p sensitizes sorafenib to hepatocellular carcinoma by targeting PAK5 mediated β-catenin/ABCB1 signaling pathway

Tong-tong Li
  Xuzhou Medical University

Jie Mou
  Xuzhou Medical University

Yao-jie Pan
  Xuzhou Medical University

Fu-chun Huo
  Xuzhou Medical University

Wen-qi Du
  Xuzhou Medical University

Jia Liang
  Xuzhou Medical University

Lin Li
  Xuzhou Medical University

Yang Wang
  Xuzhou Medical University

Dong-Sheng Pei (✉ dspei@xzhmu.edu.cn)
  Xuzhou Medical University

Abstract

Background:

Kinase inhibitor sorafenib is the first-line targeted drug for advanced hepatocellular carcinoma (HCC) patients. However, the appearance of anti-cancer agents' resistance has limited its therapeutic effect.

Methods:

In this study, quantitative real-time PCR (qPCR) and Western Blot were utilized to detect the levels of PAK5 in HCC sorafenib-resistant cells and their parental cells. The biological functions of miR-138-1-3p and PAK5 in sorafenib-resistant cells and their parental cells were explored by cell viability assay, plate colony formation assay and flow cytometric analysis. The potential mechanisms of PAK5 were evaluated via co-immunoprecipitation (co-IP), immunofluorescence, dual luciferase reporter assay and chromatin immunoprecipitation (ChIP). The effects of miR-138-1-3p and PAK5 on HCC sorafenib chemoresistant characteristics were investigated by a xenotransplantation model.

Results:

We detected significant down-regulation of miR-138-1-3p and up-regulation of PAK5 in HCC sorafenib resistance cell lines. Mechanical studies revealed that miR-138-1-3p reduced the protein expression of PAK5 by directly targeting the 3'-UTR of PAK5 mRNA. In addition, we verified that PAK5 elevated the phosphorylation and nuclear translocation of β-catenin that enhanced the transcriptional activity of multidrug resistance protein ABCB1.

Conclusions:

PAK5 contributed to the sorafenib chemoresistant characteristics of HCC by activity β-catenin/ABCB1 signaling pathway. Our findings identified the correlation between miR-138-1-3p and PAK5 and the molecular mechanisms of PAK5-mediated HCC sorafenib resistance, which provided a potential therapeutic target for advanced HCC patients.

Background

Hepatocellular carcinoma (HCC) is a malignant tumor with high fatality rate, for diagnosed patients are already at the advanced stages and hardly eligible for the curative surgical therapies [1]. Sorafenib, a multi-target tyrosine kinase inhibitor, is the Food and Drug Administration (FDA)-approved first-line targeted drug for advantage HCC patients [2, 3]. Nonetheless, sorafenib is incapable of eradicating the neoplasm [4]. Numerous patients are susceptible to sorafenib resistance for the intricate biological attributes of HCC and the activation of the compensatory signaling cascades. Sorafenib resistance has significantly constrained the therapeutic performance [5]. Identifying the resistance mechanism of sorafenib in HCC has pivotal significance, and that is likely to cause new viewpoints for the gene treatment medical experiments.

MicroRNAs (miRNAs) are putative candidate to dampen gene expressions and curb their impact at the post-transcriptional level through binding to the 3'-untranslated region (3'-UTR) of mRNAs [6, 7]. MiRNA-138-1-3p (MiR-138-1-3p) is a member of the miR-138 cluster that has been indicated as a suppressor in a diversity of tumors [8, 9]. However, the biological role of miR-138-1-3p in HCC sorafenib resistance continues ambiguity. Thus, identifying the effects of miR-138-1-3p and its targets in HCC is likely new opinions in the gene treatment. With regard to our study, we investigated the expression levels of miR-138-1-3p in HCC sorafenib-resistant cell lines and their parental cells.

P21-activated kinases 5 (PAK5) is a conserved serine/threonine protein kinase, which is well known as a modulator of cytoskeleton variations, anti-apoptosis and proliferation in cells [10]. Earlier researchers have put forward that PAK5 expression augmented in the tumor cell lines and promoted resistance of antineoplastic drugs [11, 12]. For instance, PAK5 promoted the paclitaxel chemoresistance in the epithelial ovarian cancer, and inhibiting the cisplatin-induced apoptosis in the hepatocellular carcinoma cells [13, 14]. For ourstudies, miR-138-1-3p was capable of suppressing PAK5 expression and PAK5 overexpression partly eliminated the effects of miR-138-1-3p in HCC cells.

Wnt/β-catenin signaling pathway as an evolutionarily conserved signaling pathway not just participates in embryogenesis, but also in cancer cell survival, invasion, migration and multidrug-chemoresistance [15, 16]. P-glycoprotein refers to an ATP-binding Cassette (ABC) efflux transporter distributing on the cell membrane extensively. Functionally, p-glycoprotein shares a protective mechanism to promote tumor cells survival by the efflux of intracellular drug [17]. High expression of PAK5 and ABCB1 was detected in the HCC sorafenib resistance cell lines. In mechanism analysis, PAK5 elevated the phosphorylation and nuclear translocation of β-catenin. Then, the nucleus β-catenin rendered the multidrug resistant protein ABCB1 transcriptional activation. It was indicated that miR-138-1-3p and PAK5 were critical determinants of sorafenib tolerance in HCC.

Materials And Methods

Cell culture

The human HCC cell lines HepG2, Hep3B and human embryonic kidney cell 293T were purchased from the Cell Bank China Academy of Sciences (Shanghai, China). HepG2, Hep3B and HEK293T cells were cultured in Dulbecco's modified Eagle's medium (Hyclone) supplemented with 10% (v/v) FBS. All cells were cultivated at 37 °C with 5% CO_2.

Generation of drug-resistant cells

Hep3B and HepG2 were cultures with sorafenib at the concentration of 10 μM for 48h. Viable cells remaining continue to treat with sorafenib concentration increasingly. When the resistant drug index examined up to 3 that cell lines were considered to be sorafenib resistant.

Transfection and stable cell line generation

The miR-138-1-3p mimics, mimics-NC, miR-138-1-3p inhibitor, inhibitor-NC (miR-138-1-3p, 5'-GCUACUUCACAACACCAGGGCC-3') and PAK5 siRNA (si-PAK5, 5'-CAAAGTCTTCGTACCTGAATC-3') were obtained from GenePharma (Shanghai, China). They were transfected in Hep3B and HepG2 cells using siLentFect Lipid Reagent (Bio-Rad, Hercules, CA, USA). The PAK5/Vector and Myc-PAK5 expression plasmids were purchased from Guangzhou FulenGen Co. Hep3B and HepG2 cells transiently transfected with PAK5 plasmids using X-tremeGENE HP DNA Transfection Reagent (Roche, Indianapolis, IN, USA). All transfection procedure follows the manufacturer's instructions. The LV-miR-138-1-3p-NC and LV-miR-138-1-3p (miR-138-1-3p, 5'-GCUACUUCACAACACCAGGGCC-3') were established by GenePharma (Shanghai, China). HepG2 transfected with lentivirus for 48 h, and then selected via puromycin (Vicmed, China) for 30 days.

Cell viability assay

Cell viability was assayed by the Cell Counting Kit-8 (CCK-8) kit (Beyotime, China). Post-treatment Hep3B and HepG2 cells (2×10^3) were cultured in 96-well microplate (Corning Incorporated, NewYork, USA) in quintuplicate at 37 °C with 5% CO^2. Then, CCK-8 reagent (10 µl) and 90µl serum-free medium added to each well at 24, 48, 72, and 96 hours, respectively. Measure the absorbance at 450 nm after incubated for 1 hours at 37 °C by a multi-function enzyme-linked analyzer (Biotek Instruments, Winooski, VT, USA).

RNA isolation, reverse transcription and quantitative real-time PCR (qRT-PCR)

Total RNA isolation used Trizol Reagent (Takara, Dalian, China) following the manufacturers' instructions. RNA reverse transcription performed with the PrimeScript™ RT reagent Kit (Perfect Real Time) (Takara, Dalian, China) and program set according to the operating instructions. MiRNA levels determination utilized the BrightGreen Express 2X qPCR MasterMix (Abm, Canada) with a 7500 Real-time PCR System (Life Technologies, NY, USA). Relative quantitation of miR-138-1-3p (forward: 5'-CGCGGCTACTTCACAACACC-3', reverse: 5'-AGTGCAGGGTCCGAGGTATT-3') was normalized to U6 (forward: 5'-GCTTCGGCAGCACATATACTAAAAT-3', reverse: 5'-CGCTTCACGAATT TGCGTGTCAT-3') levels, PAK5 (forward: 5'-GGC GTCCTCTTGTGTCTTC-3', reverse: 5'-GTACTGAGTCCTTCTGATTTGC-3'). ABCB1 (forward: 5'-GGCCTAATGCCGAACACATT-3', reverse: 5'-CAGCGTCTGGCCCTTCTTC-3'), ABCG2 (forward: 5'-CAGGTGGAGGCAAATCTTCGT-3', reverse 5'-ACACACCACGGATAAACTGA-3'), LRP (forward: 5'-GTCTTCGGGCCTGAGCTGGTGTCG-3', reverse 5'-CTTGGCCGTCTCTTGGGGGTCCTT-3') and MRP2 (forward: 5'-CCAAAGACAACAGCTGAAA-3', reverse 5'-TACTTGGTGGCACATAAAC-3') were normalized to GAPDH (forward: 5'-TGGTATCGTGGAAGGACTCAT-3', reverse: 5'-ATGCCAGTGAGCTTCCCGTTCAGC-3') levels (Sangon, Shanghai, China). The relative RNA expression was calculated via the comparative threshold cycle (Ct) method (relative geneexpression = 2-(ΔCtsample − ΔCtcontrol)).

Plate colony formation assay

Equal numbers of post-treatment Hep3B and HepG2 single-cell suspension cells seeded into 6-well plates and cultured for 2 weeks with 5µM sorafenib fixed in the medium. 4% paraformaldehyde fixed the clones for 15 min, and then 0.1% crystal violet stained clones for 20 min.

Flow cytometric analysis

Post-treatment Hep3B and HepG2 cells were resuspended in PBS. Annexin V-FITC Apoptosis Detection Kit (Beyotime, China) and flow cytometry (Becton Dickinson, Franklin Lakes, NJ, USA) were visualized to evaluate the percentage of apoptotic cells. Data were analyzed using a FACSCalibur Flow Cytometer (Becton Dickinson).

Antibodies and Western Blot

Cells lysis and total protein extraction were using the RIPA lysis buffer (KeyGen BioTECH, Jiangsu, China) and protein concentrations gauged by Enhanced BCA Protein Assay Kit (KeyGen BioTECH). Nuclear and cytoplasmic protein was distilled via Nuclear and Cytoplasmic Protein Extraction Kit (KeyGen BioTECH). SDS-PAGE electrophoresis and nitrocellulose blotting membranes (thermo fisher scientific) were used to proteins transfer. The specific primary antibodies incubation overnight at 4 °C, including anti-PAK5 (1:1000, Abcam, Shanghai, China), anti-ABCB1 (1: 500, Abcam, Shanghai, China), anti-β-catenin (1:1000, Santa Cruz, USA), anti-p-β-catenin (S675) (1:1000, Cell Signaling Technology, USA) and β-actin (1:5000, proteintech, China). Anti-rabbit HRP or Anti-Mouse HRP (1:10,000, Vicmed) incubated at room temperature for 2 hours afterwards. The Western Blot images were detected via Chemistar™ High-sig ECL Western Blot Substrate (Tanon, shanghai, China).

Rhodamine 123 efflux assay

Rhodamine 123 throughly dissolved in DMSO at a concentration of 5 mol/L. Seed post-treatment cells on Glass Bottom Culture Dishes (NEST, Wuxi, China) one day in advance. 5 μM Rho123 added to the medium and incubated for 30 min at 37 °C with 5%CO^2. Transpose new complete medium. Images were observed by immunofluorescence confocal laser scanning microscopy (Zeiss LSM 880).

Immunofluorescence

Seed post-treatment cells on Glass Bottom Culture Dishes (NEST, Wuxi, China) one day in advance. Cells were fixed with 4% paraformaldehyde 20 min, and then blocked with TBS (0.3% Triton X-100 and 0.25% BSA) at room temperature for 2 hours. Afterwards, they were incubated overnight at 4 °C with a primary antibody: anti-PAK5 (1:100, Abcam, Shanghai, China) and β-catenin (1:100, Santa Cruz, USA) Afterwards, they were washed three-fold with PBD. Stained with fluorescent secondary antibody: CoraLite488−conjugated Affinipure Goat Anti-Mouse IgG(H+L) and CoraLite594−conjugated Goat Anti-Rabbit IgG(H+L) (1:200, proteintech, China) at room temperature for 60 min. Nuclei were deal with 4′, 6-Diamidino-2-phenylindole (DAPI) (KeyGen BioTECH) for 10 min. Pictures were taken by immunofluorescence confocal laser scanning microscopy (Zeiss LSM 880).

Co-immunoprecipitation (co-IP)

Cells were lysed in IP lysed buffer (KeyGen BioTECH) with cocktail of protease/phosphatase inhibitors (1:100, Sigma Aldrich, MO, USA), and then added anti-β-catenin (1:100, Santa Cruz, USA) and Mouse IgG

(Beyotime) incubation overnight at 4 °C. 40 µl Protein A/G beads (Santa Cruz) were used to bind to antibodies. Wash beads and heat with 2×loading buffer. Immunoprecipitated proteins were examined by Western Blot.

Chromatin immunoprecipitation (ChIP)

CHIP assay kit (Cell Signaling Technology) was employed for CHIP assay. 1×10^7 cells were prepared for the first-step. Then DNA complexes were immunoprecipitated with β-catenin antibody. The resulting precipitated DNA samples were quantified by real-time PCR.

Luciferase reporter assay

The luciferase PAK5/Vector pGL3-Basic and pGL3-ABCB were co-transfected into Hep3B and HepG2 cells that splited in the 48-well plates by using X-tremeGENE HP DNA Transfection Reagent (Roche, Indianapolis, IN, USA). Renilla luciferase activate as normalization. Relative luciferase activity was detected 48 h after transfection following manufacturer's instructions (Promega, USA) using an Orion Microplate Luminometer (Berthold Detection System).

Xenograft transplantation model

The 4-6 weeks BALB/c female nude mice were customized by HFK Bioscience (Beijing, China) and randomized into four groups (n=6 for each): hypodermic inject $2×10^6$ LV-ctrl-HepG2-R cells; hypodermic inject $2×10^6$ LV-ctrl-HepG2-R cells and oral sorafenib 30 mg/kg, twice a day; hypodermic inject $2×10^6$ LV-mimics-HepG2-R cells and oral sorafenib 30 mg/kg, twice a day; hypodermic inject $2×10^6$ LV-siPAK5-mimics-HepG2-R and oral sorafenib 30 mg/kg, twice a day. 2 months thereafter, mice were sacrificed with the neoplasms for immunohistochemical staining. All animal experiments were in conformance with the ARRIVE (Animal Research: Reporting of In VivoExperiments) guidelines and in accordance with the National Institutes of HealthGuide for the Care and Use of Laboratory Animals.

Statistical analysis

Statistical analysis was performed by SPSS 21.0 software (SPSS, USA), and images were acquired with GraphPad Prism 5 software (La Jolla, USA). The significance of the differences between the groups was evaluated by paired two-tailed Student's t-test or one-way analysis of variance (ANOVA). All results that represented were from at least three independent experiments. Quantitative RT-PCR, luciferase reporter and cell proliferation assays were performed with triplicate duplications. Data represent the mean ± standard deviation (SD). Differences were considered statistically significant when $P<0.05$ (* $P<0.05$, ** $P<0.01$, *** $P<0.001$).

Results

MiR-138-1-3p potentiated sensitivity of sorafenib to HCC.

To explore the underlying mechanisms of HCC sorafenib resistance, we have set up the sorafenib-resistant cell models by chronic exposure to sorafenib in HCC Hep3B and HepG2 cell lines. We established sorafenib-resistant cells Hep3B-R and HepG2-R. Cell viability assay, Plate colony formation assay and Flow cytometric analysis were employed to certify the disparity between sorafenib-resistant cells and their parental cells (Fig. 1A, B and C). We chose 5 µM sorafenib in clone-formation assays and 20 µM sorafenib in apoptosis analysis for the pronounced phenotypic difference. As our data indicated, the sorafenib-resistant cells possessed robust colony-formation capability and blunted to sorafenib-reduced apoptosis in comparison with their parental counterparts after exposure to sorafenib. These suggested that we have developed the stabilized sorafenib-resistant cells lines. Previous reports highlighted the fact that miR-138 sensitized the tumors to chemotherapies. Herein, we intended to explore the expression levels of miR-138-1-3p in HCC cell lines and drug-resistance cell lines accordingly by qRT-PCR. In accordance with our results, miR-138-1-3p levels were considerably down-regulated in the drug-resistance cell lines versus their parental cells (Fig. 1D).

To investigate the effects of miR-138-1-3p in attained resistance to sorafenib in HCC cell lines, transient transfection was operated for gain and loss of function studies by miR-138-1-3p mimics and miR-138-1-3p inhibitor, respectively. The transient transfection effectiveness of miR-138-1-3p (mimics and inhibitor) in HCC Hep3B and HepG2 cells was carried out via qRT-PCR (Fig. 1E). The cell proliferation was calculated with Cell Counting Kit-8 (CCK-8) kit in transfected Hep3B and HepG2 cells at indicated sorafenib concentrations (10 µM) for 48 h. The CCK-8 assay demonstrated that miR-138-1-3p sensitized Hep3B and HepG2 cells to sorafenib treatment. Accordingly, miR-138-1-3p inhibitor significantly enhanced sorafenib resistance in Hep3B and HepG2 cells (Fig. 1F). Suggesting that miR-138-1-3p functioned as a tumor suppressor by sensitizing HCC cells to sorafenib treatment and down-regulation of miR-138-1-3p facilitated sorafenib resistance in HCC cells. Analogously, transfected Hep3B and HepG2 cells were seeded in the 6-well plates approximately 100 cells/well to assess the effect of miR-138-1-3p on clone-formation at indicated sorafenib concentrations (5 µM). The clone-formation assay indicated that inhibited miR-138-1-3p actually increased the production of the resistant colonies, whereas overexpression miR-138-1-3p apparently obstructs the clone-formation (Fig. 1G). In line with our results from clone-formation, transient transfection miR-138-1-3p mimics in Hep3B and HepG2 cells virtually dampened the rise of sorafenib-tolerance, in addition to promoting the sorafenib-mediated apoptosis, which was detected by the flow cytometric analysis. With one voice, miR-138-1-3p inhibitor interrupted the cell cytotoxicity of sorafenib (Fig. 1H). Our hypothesis for miR-138-1-3p potentiating sensitivity of sorafenib to HCC was preliminarily verified.

MiR-138-1-3p inhibited PAK5 expression by directly targeted the 3'-UTR of PAK5.

MiRNAs were merited to identify as inhibitors of protein-coding genes expression. For the purpose of throwing discussion on the molecular mechanism correlated with miR-138-1-3p in HCC sorafenib resistance and whether PAK5 was targeted in a direct manner by miR-138-1-3p, TargetScan (http://www.targetscan.org/) and miRTarBase (http://mirtarbase.mbc.nctu.edu.tw/) were employed for the prediction of the possibility. As our findings revealed, the PAK5 mRNA and protein level were markedly

increased in Hep3B and HepG2 sorafenib, ADR, 5FU resistant cells lines validated by qRT-PCR and Western Blot (Fig. 2A). Moreover, miR-138-1-3p mimics apparently down-regulated PAK5 and miR-138-1-3p inhibitor promoted PAK5 expression in Hep3B and HepG2 cells at the protein and mRNA levels (Fig. 2B). Subsequent to that, we have set three groups of co-transfection for the purpose of interrogating whether miR-138-1-3p affected HCC sorafenib resistance by means of PAK5 in Hep3B and HepG2 cell lines, and Western Blot was made for examining the co-transfection effectiveness (Fig. 2C). The application of cell viability assay was made for detecting the cell proliferation, and the data revealed the fact that following the transfection with miR-138-1-3p mimics, the declining tendency could be impaired with the help of the co-transfection with PAK5 plasmids. Inversely, the increased cell viability by miR-138-1-3p inhibitor could be eliminated after co-transfected with si-PAK5 (Fig. 2D). The peroration of plate colony formation assay was in step with cell viability (Fig. 2E). Flow cytometry was employed to analyze the effects of PAK5 and miR-138-1-3p on sorafenib-driven apoptosis in Hep3B and HepG2 cell lines. Our data demonstrated that PAK5 overexpression abolished miR-138-1-3p-induced cell apoptosis and PAK5 inhibition deleted the cytoprotection of miR-138-1-3p inhibitor following dealing with sorafenib (Fig. 2F). These suggested that miR-138-1-3p could exert an impact on the sorafenib resistance of HCC cells via PAK5.

A luciferase reporter test was put to confirm that PAK5 constituted an actual target of miR-138-1-3p. The cloning of the PAK5 WT 3'-UTR (conserved wild type) or PAK5 mut 3'-UTR (conserved mutant type) was carried out into psiCHECK2 vector (psiCHECK2-PAK5 WT 3'-UTR or psiCHECK2-PAK5 mut 3'-UTR) with the upstream luciferase. Mechanically, the luciferase activities of the reporter gene in Hep3B and HepG2 cells co-transfected with psiCHECK2-PAK5 WT 3'-UTR and miR-138-1-3p mimics were significantly reduced in comparison with their control (psiCHECK2-PAK5 mut 3'-UTR or miR-138-1-3p mimics-NC) (Fig. 2G).

PAK5 eliminated the sorafenib induced cell apoptosis in HCC in vitro.

For the ulterior substantiation of the correlation of PAK5 and HCC sorafenib resistance, we made use of the PAK5/S573N (constitutively active) plasmid and PAK5/K478M (constitutively inactive) plasmid. Thereafter, we carried out four groups that transfected with PAK5/Vector, PAK5/WT, PAK5/S573N and PAK5/K478M, correspondingly, in Hep3B and HepG2 cell lines. Western Blot verified the transfection effectiveness (Fig. 3A). Particularly lower viability of PAK5/K478M-transfected cells could be observed in comparison with the PAK5/WT-transfected and PAK5/S573N-transfected cells (Fig. 3B). Furthermore, the yield of resistant colonies by the PAK5/K478M and PAK5/Vector transfection had no statistical difference in the colony formation assay. Apparently, enlarged cell colonies could be observed in the PAK5/WT- or PAK5/S573N-transfected cells (Fig. 3C). Sorafenib-triggered apoptosis was also significantly inhibited following the transiently transfection with PAK5/WT or PAK5/S573N (Fig. 3D). These findings indicate the fact that PAK5 mediated the chemotherapy tolerance of sorafenib in HCC and the sensibility increased with the constitutively inactive of PAK5.

The findings that we indicated earlier suggested that PAK5 promoted sorafenib-resistance in HCC, following that, we threw discussion on whether the knock out PAK5 in sorafenib-resistance HCC cell lines

had the potential of rehabilitating the drug susceptibility of sorafenib. We depleted the PAK5 expression in Hep3B-R and HepG2-R by small interfering RNA (siRNA), and the interference efficiency was confirmed with the help of the Western Blot (Fig. 3E). Thereafter, we calculated the absorbance at 450 nm, confirming that the cell viability of interfere group was evidently reduced compared with sorafenib-resistance subpopulation, meanwhile higher than their parental cells (Fig. 3F). Identically, ablation of PAK5 also obstructed the yield of resistant colonies following the sorafenib treatment (Fig. 3G). Besides that, the steady knockdown of PAK5 stimulated the apoptosis of drug-tolerant cells to sorafenib (Fig. 3H). To conclude, PAK5 was needed for the viability of the drug-tolerant subpopulation, and PAK5 was likely to constitute a potential therapy target for HCC sorafenib resistance patients.

PAK5 promoted ABCB1 transcriptional activation via Wnt/β-catenin signaling pathway.

In the start, we performed the screening of a number of multidrug resistance proteins, aimed at investigating the expression profile in Hep3B-R, HepG2-R and their parental cells, included ABCB1, ABCG2, LRP and MRP2. The Western Blot revealed a prominently augment of ABCB1 exceeding the other MDR genes in the sorafenib-tolerant subpopulation (Fig. 4A). In a bid to determine the functional operation of P-gp in the sorafenib-tolerant cells, we took advantage of the fluorescent dye rhodamine 123 (Rho123) as an index to test the P-gp activity. Following a period of 30 min, just 10% initial Rh123 fluorescence retained in the intracellular compartment of Hep3B-R and HepG2-R, whereas in their parental cells approximately 60%. This was observed as consistent with the Western Blot data. Besides that, PAK5/WT-transfected and PAK5/S573N-transfected cells also hold a higher efflux of Rh123 fluorescence in compared with the transfection of PAK5/K478M and PAK5/Vector, which indicated that PAK5 was likely to augment the ABCB1 expression in HCC cell lines (Fig. 4B).

PAK5 has been indicated to phosphorylate Pacsin1 and Synaptojanin1 as promoting the vesicle transport in nerve cells [18]. Protein structure prediction of β-catenin has made it clear that there was a PAK5-related identical sequence (K/R) (R/X) X(S/T) in it, and serine 675 constituted quite a potential PAK5 phosphorylation site [19, 20]. To certify the underlying mechanisms, we performed co-IP assay. Endogenous interaction of PAK5 and β-catenin could be detected in Hep3B cells and more remarkable in sorafenib-tolerant cells (Fig. 4C). Our Western Blot assay also confirmed it. We transfected the PAK5/Vector, PAK5/WT, PAK5/S573N and PAK5/K478M, correspondingly in Hep3B and HepG2 cell lines for the investigation of the protein expression level of ABCB1, β-catenin and p-β-catenin (S675). High expression of ABCB1 and p-β-catenin (S675) was detected in PAK5/WT- and PAK5/S573N-transfected cells, but β-catenin not altered (Fig. 4D). Also, we could observe similar variations in Hep3B-R and HepG2-R cells in comparison with their parental cells (Fig. 4E). On the other hand, the expression of ABCB1 and p-β-catenin (S675) were blunted with knocked down PAK5 by small interfering RNA in Hep3B-R and HepG2-R cells (Fig. 4F). For testing a particular modulation of PAK5 on β-catenin signaling pathway, the co-transfection of PAK5/Vector, PAK5/WT, PAK5/S573N, PAK5/K478M severally with β-catenin or β-catenin/S675A (constitutively inactive) performed on the human embryonic kidney HEK-293T cells in accordance with Fig. 4G. Additionally, these observations verified that PAK5 up-regulated ABCB1 expression via the Wnt/β-catenin signaling pathway (Fig. 4G).

PAK5 facilitated the nuclear translocation of β-catenin.

For investigating the latent process of PAK5 in the Wnt/β-catenin signaling pathway activity, we manipulated the nuclear and cytoplasmic fractionation to test the cellular distribution of β-catenin and p-β-catenin (S675) in Hep3B and HepG2 cell lines after transfected PAK5/Vector, PAK5/WT, PAK5/S573N and PAK5/K478M plasimids, correspondingly. As our findings revealed, PAK5/WT and PAK5/S573N powerful facilitated the nuclear distribution of β-catenin and p-β-catenin (S675), and hardly changed detected in PAK5/K478M-transfected cells, which compared with the PAK5/Vector group (Fig. 5A). We also stressed the distribution of β-catenin and p-β-catenin (S675) in Hep3B-R and HepG2-R cells, sharing similarity with PAK5 overexpression (Fig. 5B). Furthermore, silence of PAK5 particularly reduced the phosphorylation of β-catenin and nuclear allocation of p-β-catenin (S675) in Hep3B-R and HepG2-R cells. In brief, the dynamically relocation of β-catenin and p-β-catenin could be curbed after knocked out PAK5 (Fig. 5C).

Consistently, as immunofluorescence indicated, the positive signal (red) of PAK5 was strikingly higher in the cytoplasm in PAK5/WT, PAK5/S573N and PAK5/K478M-transfected cells in comparison with the weak staining in control cohorts, illustrating the transfection efficiency of PAK5. Meanwhile, there was an increase in the positive signal (green) of β-catenin in the nucleus of the PAK5/WT and PAK5/S573N-transfected cells predominantly. Like always, there was no perceptible change observed in the PAK5/K478M-transfected cells (Fig. 5D). Evidently, we were capable of detecting the robust positive signal (red) of PAK5 in the cytoplasm and positive signal (green) of β-catenin in the nucleus of Hep3B-R and HepG2-R as compared with their parental cells (Fig. 5E). All demonstrated that PAK5 elevated the phosphorylation and nuclear translocation of β-catenin.

β-catenin targeted ABCB1 promoter and actived ABCB1 transcription.

In the canonical Wnt/β-catenin signaling pathway, β-catenin translocated into nuclear to regulate the activaty of many target genes. To detect the underlying mechanism of β-catenin in HCC sorafenib resistance, CHIP with β-catenin antibody in Hep3B and HepG2 cells treated with ABCB1, ABCG2, LRP and MRP2 was employed to scrutinize the target genes. Verifying the correctness of our previous result, ABCB1 was a target gene of β-catenin and significantly increased in HCC sorafenib resistance cell lines (Fig. 6A). To evidence that β-catenin is directly active ABCB1 transcription, we made use of the pGL3-ABCB1 and pGL3-basic plasmids to measure ABCB1 promoter activity as a result of β-catenin nuclear translocation in accordance with a dual luciferase reporter assay. There was a markedly luciferase activity in the cells that transfected β-catenin plasmid, but not in cells that were transfected β-catenin/S675A (constitutively inactive) plasmid. Also, a transcriptional activity could be identified as co-transfected with PAK5 (Fig. 6B and C). These findings again stressed the fact that the PAK5-mediated β-catenin phosphorylation promotes the transcriptional activity of ABCB1.

MiR-138-1-3p sensitized sorafenib to HCC by targeting PAK5 in vivo.

To further evaluate the role of miR-138-1-3p and PAK5 in HCC sorafenib resistance *in vivo*, xenograft cancer models were established by subcutaneously inoculating HepG2-R cells. The nude mice were randomly assigned into four groups (n = 6 for each): LV-ctrl-HepG2-R cells (NC), LV-ctrl-HepG2-R cells and oral sorafenib (Ctrl), LV-miR-138-1-3p-HepG2-R cells and oral sorafenib (miR-138-1-3p), LV-shPAK5-HepG2-R and oral sorafenib (shPAK5). After tumor growth reached a volume of 100 mm^3, the last three groups' mice begun to oral sorafenib 30 mg/kg, twice a day as well as the first group mice treated with placebo. Compared with miR-138-1-3p overexpressed and PAK5 inhibited xenografted tumors, the size and weight of NC and Ctrl groups' tumors were increased significantly. But no statistical difference in LV-ctrl-HepG2-R groups whether oral sorafenib or not (Fig. 7A, B and C). Immunohistochemical assay was played in the xenograft tissues that isolated from nude mice. In line with our *in vitro* experiment, miR-138-1-3p overexpressed xenografted tumors, PAK5 and ABCB1 positive signal dampened entirely. Concordantly, in PAK5 inhibited xenografted tumors, ABCB1 positive signal also subdued (Fig. 7D).

Discussion

HCC is the fourth leading cause of the global cancer deaths. Surgical resection or liver transplantation is considered as the preferred therapy for HCC patients. Nonetheless, a majority of the HCC patients had missed the best treatment time due to the concealed onset, fast-paced progress and high malignancy [21]. Sorafenib is naturally emerging as a pivotal part of HCC treatment, but the clinical response to sorafenib is seriously limited by drug resistance [22]. Our works aimed at examining the cellular alterations and the molecular mechanisms of sorafenib resistance. Studies placed on cancer drugs acquired resistance mainly included four aspects: ATP-binding cassette (ABC) proteins, epithelial-mesenchymal transition (EMT), cancer stem cells (CSCs), and hypoxia-inducible factor (HIFs) mediated chemotherapy resistance [23–27]. MiRNAs were wildly studied for the inhibition of target genes [28, 29]. MiRNA-138-1-3p is a member hailing of the miR-138 family. Both the MiR-138-1 and miR-138-2 clusters are responded in the entirely identical mature miRNA sequences, which are located on the chromosomes 3p21.33 and 16q13, correspondingly [30, 31]. The dynamic modulation of miR-138 has been detected in the multiple kinds of disease mechanisms, for instance, type-2 diabetes, rheumatoid arthritis, early-onset Alzheimer's disease and cancers [32–35]. Moreover, miRNA-138-5p has been indicated as a reverse factor of gefitinib resistance by inhibiting GPR124 (G protein-coupled receptor 124) expression in NSCLC (non-small cell lung cancer) cells [36]. Besides, low expression of miR-138-5p was detected in CRC (human colorectal cancer) and bladder tissues [37, 38]. It was of interest that we investigated the functional interaction of miR-138-1-3p in HCC sorafenib resistance.

For the current study, we figured out the potential sequestration of miR-138-1-3p in HCC sorafenib-tolerant cells that underlining the significance of miR-138-1-3p in liver homeostasis. Moreover, the sensitivity of sorafenib to HCC apparently augmented after transiently transfected with miR-138-1-3p mimics in Hep3B and HepG2 cell lines. Then, we made use of the miRNA target prediction databases TargetScan (http://www.targetscan.org/) and miRTarBase (http://mirtarbase.mbc.nctu.edu.tw/) for the prediction of the miR-138-1-3p target genes, PAK5 has brought our attention for the specific up-regulation in sorafenib-

resistant cells. Luciferase reporter assay suggested that miR-138-1-3p dampened PAK5 expression via directly targeting the 3'-UTR of PAK5. And overexpression PAK5 might alleviate sorafenib cytotoxicity of HCC cells. We first validated PAK5 as a target of miR-138-1-3p.

PAKs preliminarily were identified as the ligands for small (21 kDa) GTPases Rac1 and Cdc42. The PAKs family (PAK1-PAK6) includes two subfamilies: subfamily I (PAK1-PAK3) and subfamily II (PAK4-PAK6). The family members that we emphasize, PAK5 (also named PAK7), is the latest member of the PAK family [39]. Numerous studies have indicated that PAKs essentially contributed to cytoskeleton and cell motility, more than that, they also involved in diverse kinds of signal pathways that over-activity in cancers. Provided the essential role that PAKs performs in normal cellular homeostasis, it is of no surprise that PAKs are capable of interacting with the potent oncogenic systems [40]. Former studies confirmed the fact that PAK5 constituted a key signaling molecule in cancer cells, which involved modulating tumorigenesis, anti-apoptosis and anti-cancer agents' tolerance. In the current study, we investigated significant PAK5 up-regulation in drug-tolerant subpopulation (Hep3B-ADR, Hep3B-5FU, Hep3B-R, HepG2-ADR, HepG2-5FU, and HepG2-R). Moreover, a potential driver of sorafenib-induced cell apoptosis was detected after we attenuate PAK5 expression by small interference RNA in sorfenib-tolerant subpopulation. This suggested that alleviating PAK5 expression facilitated sorafenib-induced cell apoptosis and disrupted the tolerance of sorafenib in sorafenib-tolerant cells. Taken together, HCC cells circumvented the sorafenib-induced cellular damage by PAK5-mediated survival pathways. PAK5 seemed as a new therapeutic target, interfering with the development and survival of the sorafenib-tolerant HCC cells.

ATP-binding cassette (ABC) transporters are important cellular protection mechanisms after treat with sorafenib [41]. We took advantage of the fluorescent dye rhodamine 123 (Rho123) as an index to test the P-gp activity. Following a period of 30 min, less Rh123 fluorescence retained in Hep3B-R and HepG2-R cells than their parental cells. We performed the screening of multidrug resistance proteins, ABCB1, ABCG2, LRP and MRP2 were the most extensively studied in HCC [42−45]. Our present results showed prominently augment of ABCB1 exceeding the other MDR genes in sorafenib-tolerant subpopulation. Furthermore, transiently transfected PAK5 wild-type or active-type plasmid apparently increased ABCB1 expression and attenuated Rh123 fluorescence stain in HCC cells. These findings hinted that PAK5 might contribute to gain sorafenib resistance by affecting the expression of ABCB1 in HCC cells.

We further elucidated how PAK5 regulated ABCB1 expression in HCC sorafenib-tolerant cells. Studies indicated that β-catenin serine 675 is a promising PAK5 phosphorylation site, and the activation of the Wnt/β-catenin signaling pathway could promote lung adenocarcinoma cisplatin resistance by regulating ABC transporter expression [46, 47]. These have provided a new perspective for our study. We tested the protein level of p-β-catenin (S675) in sorafenib-tolerant cells and their parental cells, clearly up-regulation in the former. Besides, altering the PAK5 expression apparently influenced the protein expression of p-β-cateninm (S675) in parental cells. Based on mechanisms assays, we demonstrated that PAK5 may activate the β-catenin signaling pathway by promoting β-catenin (S675) phosphorylation and nuclear

translocation. Subsequent to that, the accumulated β-catenin promoted ABCB1 transcription by binding to ABCB1 promoter directly.

Conclusions

To conclude, our findings have demonstrated that miR-138-1-3p performed the negative regulation of the PAK5 expression, and PAK5-mediated sorafenib-tolerance HCC cells. Up-regulated PAK5 in sorfenib-tolerant subpopulation had a significant correlation with the HCC cell escapism sorafenib lethality. The combination analysis of miR-138-1-3p and PAK5 could be employed for the purpose of predicting the sorafenib tolerance, and providing the individualized therapy strategies in HCC patients.

Abbreviations

HCC, hepatocellular carcinoma;

FDA, Food and Drug Administration;

MiRNAs, MicroRNAs;

PAK5, P21-activated kinases 5;

ABC, ATP-binding Cassette;

qRT-PCR, quantitative real-time PCR;

co-IP, Co-immunoprecipitation;

CHIP, Chromatin immunoprecipitation.

Declarations

Ethics approval and consent to participate

Animal experiments were in conformance with the Institutional Animal Care and Use Committee of Xuzhou Medical University.

Consent for publication

Not applicable.

Availability of data and materials

All data generated or analyzed during the current study are available from the corresponding author on reasonable request.

Conflicts of interest

All authors declare no conflicts of interest.

Authors' contributions

TT Li, J Mou and DS Pei designed, performed and analyzed experiments. YJ Pan, FC Huo, WQ Du, J Liang, L Li and Y Wang performed experiments. TT Li and J Mou wrote the paper. DS Pei commented on the study and revised the paper. DS Pei obtained funding and designed the research. All authors read and approved the final manuscript.

References

1. Makol A, Kaur H, Sharma S, Kanthaje S, Kaur R, Chakraborti A. Vimentin as a potential therapeutic target in sorafenib resistant HepG2, a HCC model cell line. Clin Mol Hepatol. 2020 Jan;26(1):45–53.

2. Zheng JF, He S, Zeng Z, Gu X, Cai L, Qi G. PMPCB Silencing Sensitizes HCC Tumor Cells to Sorafenib Therapy. Mol Ther. 2019 Oct;27(10)(2):1784–95.

3. Llovet JM, Decaens T, Raoul JL, Boucher E, Kudo M, Chang C, et al. Brivanib in patients with advanced hepatocellular carcinoma who were intolerant to sorafenib or for whom sorafenib failed: results from the randomized phase III BRISK-PS study. J Clin Oncol. 2013 Oct 1;31(28):3509-16.

4. Tong M, Che N, Zhou L, Luk ST, Kau PW, Chai S, et al. Efficacy of annexin A3 blockade in sensitizing hepatocellular carcinoma to sorafenib and regorafenib. J Hepatol. 2018 Oct;69(4):826–39.

5. Wu CX, Wang XQ, Chok SH, Man K, Tsang SHY, Chan ACY, et al. Blocking CDK1/PDK1/β-Catenin signaling by CDK1 inhibitor RO3306 increased the efficacy of sorafenib treatment by targeting cancer stem cells in a preclinical model of hepatocellular carcinoma. Theranostics. 2018 Jun 13;8(14):3737–3750.

6. Gong H, Song L, Lin C, Liu A, Lin X, Wu J, et al. Downregulation of miR-138 sustains NF-κB activation and promotes lipid raft formation in esophageal squamous cell carcinoma. Clin Cancer Res. 2013 Mar 1;19(5):1083-93.

7. Wang Y. MicroRNA and cancer–focus on apoptosis. J Cell Mol Med. 2009 Jan;13(1):12–23.

8. Pan X, Chen Y, Shen Y, Tantai J. Knockdown of TRIM65 inhibits autophagy and cisplatin resistance in A549/DDP cells by regulating miR-138-5p/ATG7. Cell Death Dis. 2019 Jun 3;10(6):429.

9. Zhao X, Yang L, Hu J. miR-138 might reverse multidrug resistance of leukemia cells. Leuk Res. 2010 Aug;34(8):1078–82.

10. Geng N, Li Y, Zhang W, Wang F, Wang X, Jin Z, et al. A PAK5-DNPEP-USP4 axis dictates breast cancer growth and metastasis. Int J Cancer. 2020 Feb;15(4):1139–51. 146(.

11. Kumar R, Sanawar R, Li X. Structure, biochemistry, and biology of PAK kinases. Gene. 2017;605:20–31.

12. Wang XX, Cheng Q, Zhang SN, Qian HY, Wu JX, Tian H, et al. PAK5-Egr1-MMP2 signaling controls the migration and invasion in breast cancer cell. Tumour Biol. 2013 Oct;34(5):2721–9.

13. Li D, Yao X. The overexpression of P21-activated kinase 5 (PAK5) promotes paclitaxel-chemoresistance of epithelial ovarian cancer. Tumour Biol. 2015 May;36(5):3685–91.

14. Zhang DG, Zhang J, Mao LL, Wu JX, Cao WJ, Zheng JN. p21-Activated kinase 5 affects cisplatin-induced apoptosis and proliferation in hepatocellular carcinoma cells. Tumour Biol. 2015 May;36(5):3685–91.

15. Huelsken J. The Wnt signalling pathway. J Cell Sci. 2002;115:3977–8.

16. Toh TB, Lim JJ, Hooi L, Rashid MBMA, Chow EK. Targeting Jak/Stat pathway as a therapeutic strategy against SP/CD44$^+$ tumorigenic cells in Akt/β-catenin-driven hepatocellular carcinoma. J Hepatol. 2020 Jan;72(1):104–18.

17. Chen N, Kong Y, Wu Y, Gao Q, Fu J, Sun X, et al. CAC1 knockdown reverses drug resistance through the downregulation of P-gp and MRP-1 expression in colorectal cancer. PLoS One. 2019 Sep;10(9):e0222035. 14(.

18. Strochlic TI, Concilio S, Viaud J, Eberwine RA, Wong LE, Minden A, et al. Identification of neuronal substrates implicates Pak5 in synaptic vesicle trafficking. Proc Natl Acad Sci U S A. 2012;109:4116–21.

19. Gu X, Wang C, Wang X, Ma G, Li Y, Cui L, et al. Efficient inhibition of human glioma development by RNA interference-mediated silencing of PAK5.Int. J Biol Sci. 2015;11:230–7.

20. Zhe-ping Fang ,Bei-ge Jiang. Gu Xue-feng, Zhao B, Ge Rui-liang. Fa-biao Zhang. P21-activated kinase 5 plays essential roles in the proliferation and tumorigenicity of human hepatocellular carcinoma. Acta Pharmacol Sin 2014; 35:82–8.

21. Song Z, Liu T, Chen J, Ge C, Zhao F, Zhu M, et al. HIF-1α-induced RIT1 promotes liver cancer growth and metastasis and its deficiency increases sensitivity to sorafenib. Cancer Lett. 2019;460:96–107.

22. Wang C, Wang H, Lieftink C, du Chatinier A, Gao D, Jin G, et al. CDK12 inhibition mediates DNA damage and is synergistic with sorafenib treatment in hepatocellular carcinoma. Gut. 2020 Apr;69(4):727–36.

23. Tandia M, Mhiri A, Paule B, Saffroy R, Cailliez V, Noé G, et al. Correlation between clinical response to sorafenib in hepatocellular carcinoma treatment and polymorphisms of P-glycoprotein (ABCB1) and of breast cancer resistance protein (ABCG2): monocentric study. Cancer Chemother Pharmacol. 2017;79:759–66.

24. Hu B, Cheng JW, Hu JW, Li H, Ma XL, Tang WG, et al. KPNA3 Confers Sorafenib Resistance to Advanced Hepatocellular Carcinoma via TWIST Regulated Epithelial-Mesenchymal Transition. J Cancer. 2019;10:3914–25.

25. Mir N, Jayachandran A, Dhungel B, Shrestha R, Steel JC. Epithelial-to-Mesenchymal Transition: A Mediator of Sorafenib Resistance in Advanced Hepatocellular Carcinoma. Curr Cancer Drug Targets. 2017;17:698–706.

26. Fan Z, Duan J, Wang L, Xiao S, Li L, Yan X, et al. PTK2 promotes cancer stem cell traits in hepatocellular carcinoma by activating Wnt/β-catenin signaling. Cancer Lett. 2019;450:132–43.

27. Méndez-Blanco C, Fondevila F, García-Palomo A, González-Gallego J, Mauriz JL. Sorafenib resistance in hepatocarcinoma: role of hypoxia-inducible factors. Exp Mol Med. 2018 Oct 12;50(10):1–9.

28. Wang Y. MicroRNA and cancer–focus on apoptosis.J Cell Mol Med 2009; 1582–4934.

29. Mizuno T, Chou MY. A unique mechanism regulating gene expression: translational inhibition by a complementary RNA transcript (micRNA). Proc Natl Acad Sci U S A. 1984;81:1966–70.

30. Wang W, Zhao LJ, Tan YX, Ren H, Qi ZT. MiR-138 induces cell cycle arrest by targeting cyclin D3 in hepatocellular carcinoma. Carcinogenesis. 2012;33:1113–20.

31. Liu X, Jiang L, Wang A, Yu J, Shi F, Zhou X. MicroRNA-138 suppresses invasion and promotes apoptosis in head and neck squamous cell carcinoma cell lines. Cancer Lett. 2009;286:217–22.

32. Nunez Lopez YO, Retnakaran R, Zinman B, Pratley RE, Seyhan AA. Predicting and understanding the response to short-term intensive insulin therapy in people with early type 2 diabetes. Mol Metab. 2019;20:63–78.

33. Shao L. miR-138 activates NF-κB signaling and PGRN to promote rheumatoid arthritis via regulating HDAC4. Biochem Biophys Res Commun. 2019;519:166–71.

34. Zhang HJ, Wei QF, Wang SJ, Zhang HJ, Zhang XY, Geng Q, et al. LncRNA HOTAIR alleviates rheumatoid arthritis by targeting miR-138 and inactivating NF-κB pathway. Int Immunopharmacol. 2017;50:283–90.

35. Boscher E, Husson T, Quenez O, Laquerrière A, Marguet F, Cassinari K, et al. Copy Number Variants in miR-138 as a Potential Risk Factor for Early-Onset Alzheimer's Disease. J Alzheimers Dis. 2019;68:1243–55.

36. Gao Y, Fan X, Li W, Ping W, Deng Y, Fu X. miR-138-5p reverses gefitinib resistance in non-small cell lung cancer cells via negatively regulating G protein-coupled receptor 124. Biochem Biophys Res Commun. 2014;446:179–86.

37. Zhao L, Yu H, Yi S, Peng X, Su P, Xiao Z, et al. The tumor suppressor miR-138-5p targets PD-L1 in colorectal cancer. Oncotarget. 2016;7:45370–84.

38. Yang R, Liu M, Liang H, Guo S, Guo X, Yuan M, et al. miR-138-5p contributes to cell proliferation and invasion by targeting Survivin in bladder cancer cells. Mol Cancer. 2016;15:82.

39. Geng N, Li Y, Zhang W, Wang F, Wang X, Jin Z, et al. A PAK5-DNPEP-USP4 axis dictates breast cancer growth and metastasis. Int J Cancer 2019.

40. Huo FC, Pan YJ, Li TT, Mou J, Pei DS. PAK5 promotes the migration and invasion of cervical cancer cells by phosphorylating SATB1.Cell Death Differ 2019; 26:994–1006.

41. Yang Y, Zhang J, Wu T, Xu X, Cao G, Li H,et al. Histone deacetylase 2 regulates the doxorubicin (Dox) resistance of hepatocarcinoma cells and transcription of ABCB1. Life Sci. 2019;216:200–6.

42. Li W, Sparidans R, El-Lari M, Wang Y, Lebre MC, Beijnen JH, et al. P-glycoprotein (ABCB1/MDR1) limits brain accumulation and Cytochrome P450-3A (CYP3A) restricts oral availability of the novel FGFR4 inhibitor fisogatinib (BLU-554). Int J Pharm. 2020 Jan 5;573:118842.

43. Xie ZY, Liu MS, Zhang C, Cai PC, Xiao ZH, Wang FF. Aspirin enhances the sensitivity of hepatocellular carcinoma side population cells to doxorubicin via miR-491/ABCG2. Biosci Rep. 2018 Nov;9(6):BSR20180854. 38(.

44. Zhang J, Luo N, Tian Y, Li J, Yang X, Yin H, et al. USP22 knockdown enhanced chemosensitivity of hepatocellular carcinoma cells to 5-Fu by up-regulation of Smad4 and suppression of Akt. Oncotarget. 2017;8:24728–40.

45. Chen Y, Zhao H, Li H, Feng X, Tang H, Qiu C, et al. LINC01234/MicroRNA-31-5p/MAGEA3 Axis Mediates the Proliferation and Chemoresistance of Hepatocellular Carcinoma Cells. Mol Ther Nucleic Acids. 2019;19:168–78.

46. Yun CY, You ST, Kim JH, Chung JH, Han SB, Shin EY, et al. p21-activated kinase 4 critically regulates melanogenesis via activation of the CREB/MITF and β-catenin/MITF pathways. J Invest Dermatol. 2015;135:1385–94.

47. Wang Q, Geng F, Zhou H, Chen Y, Du J, Zhang X, et al. MDIG promotes cisplatin resistance of lung adenocarcinoma by regulating ABC transporter expression via activation of the WNT/β-catenin signaling pathway. Oncol Lett. 2019;18:4294–307.
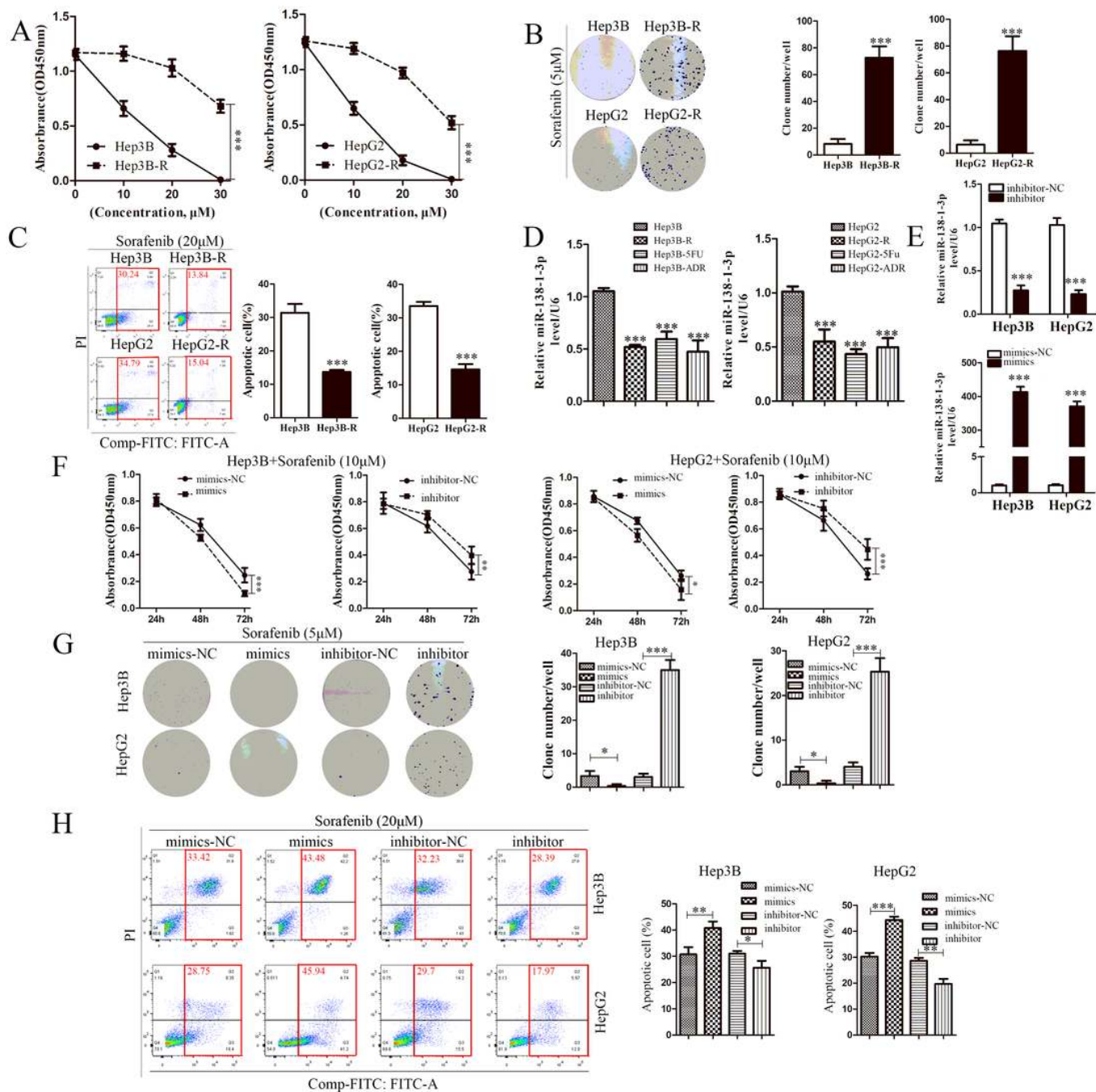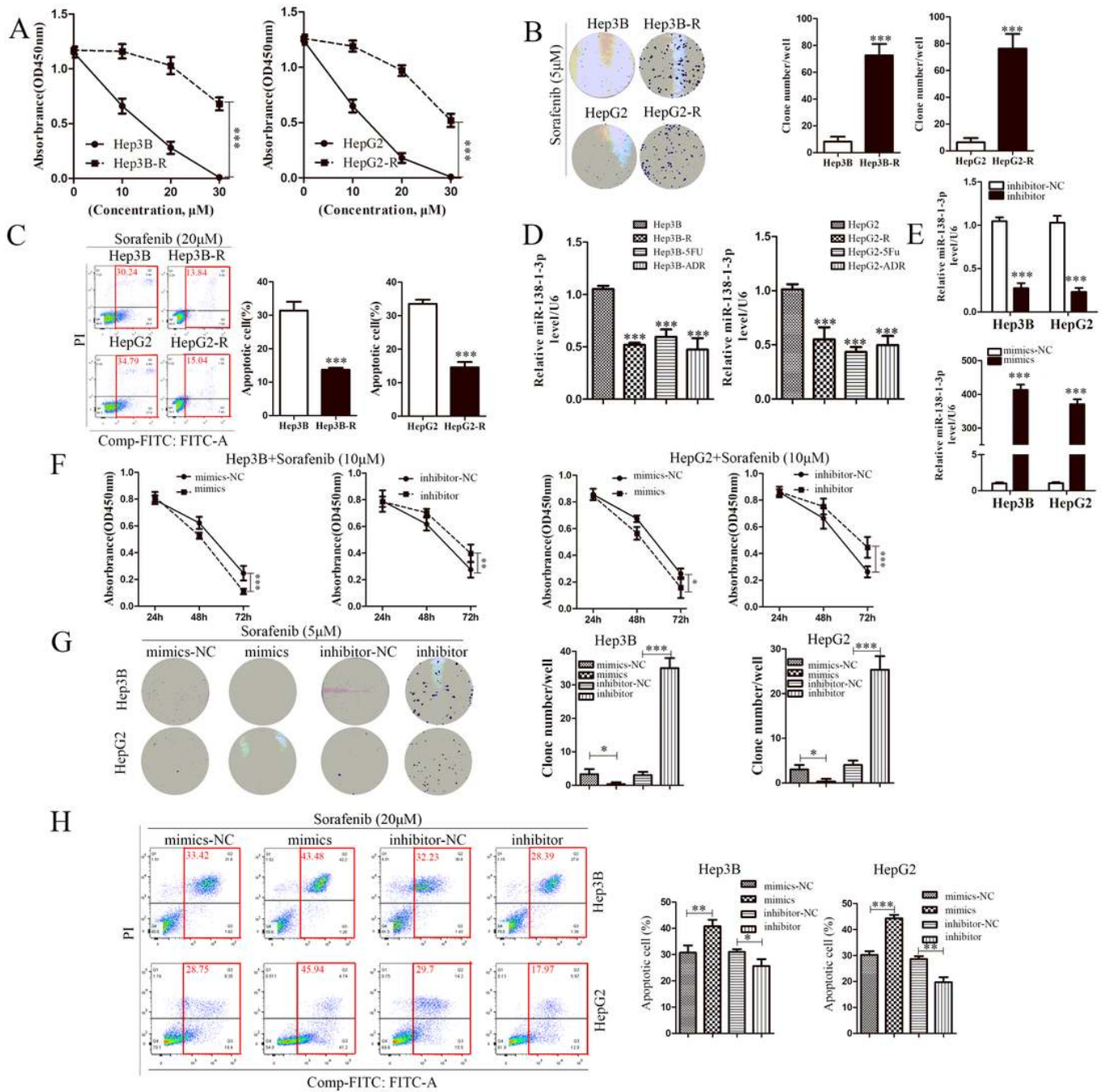
Figures

Figure 1

MiR-138-1-3p potentiated sensitivity of sorafenib to HCC. (A) CCK-8 assays in Hep3B, Hep3B-R and HepG2, HepG2-R cells after dealing with sorafenib at the concentration of 0, 10, 20, 30μM, 48hours. (B) Representative images for plate colony formation assay in Hep3B, Hep3B-R and HepG2, HepG2-R cells after dealing with sorafenib at the concentration of 5μM, 10days. (C) Representative images for flow cytometric analysis of Hep3B, Hep3B-R and HepG2, HepG2-R cells after dealing with sorafenib at the concentration of 20μM, 24hours. (D) Relative miR-138-1-3p expression in HepG2, HepG2-ADR, HepG2-5FU, HepG2-R and HepG2, HepG2-ADR, HepG2-5FU, HepG2-R cells was detected by qRT-PCR, U6 was used as an internal control. (E) Conformation of the levels of miR-138-1-3p in transient transfected Hep3B and HepG2 cell lines by qRT-PCR, after transfected with miR-138-1-3p mimics or inhibitor with respective -NC

control. (F) The cell viability was detected by CCK-8 assays after transfection of mimics or inhibitor with respective -NC control, dealing with sorafenib at the concentration of 10µM, 48hours. (G) Representative images for plate colony formation assay in Hep3B and HepG2 cells after transfection of mimics or inhibitor with respective -NC control and deal with sorafenib at the concentration of 5µM, 10days. (H) Representative images for flow cytometric analysis of HepG2 and Hep3B cell lines after transfection of mimics or inhibitor with respective -NC control and deal with sorafenib at the concentration of 20µM, 24hours.
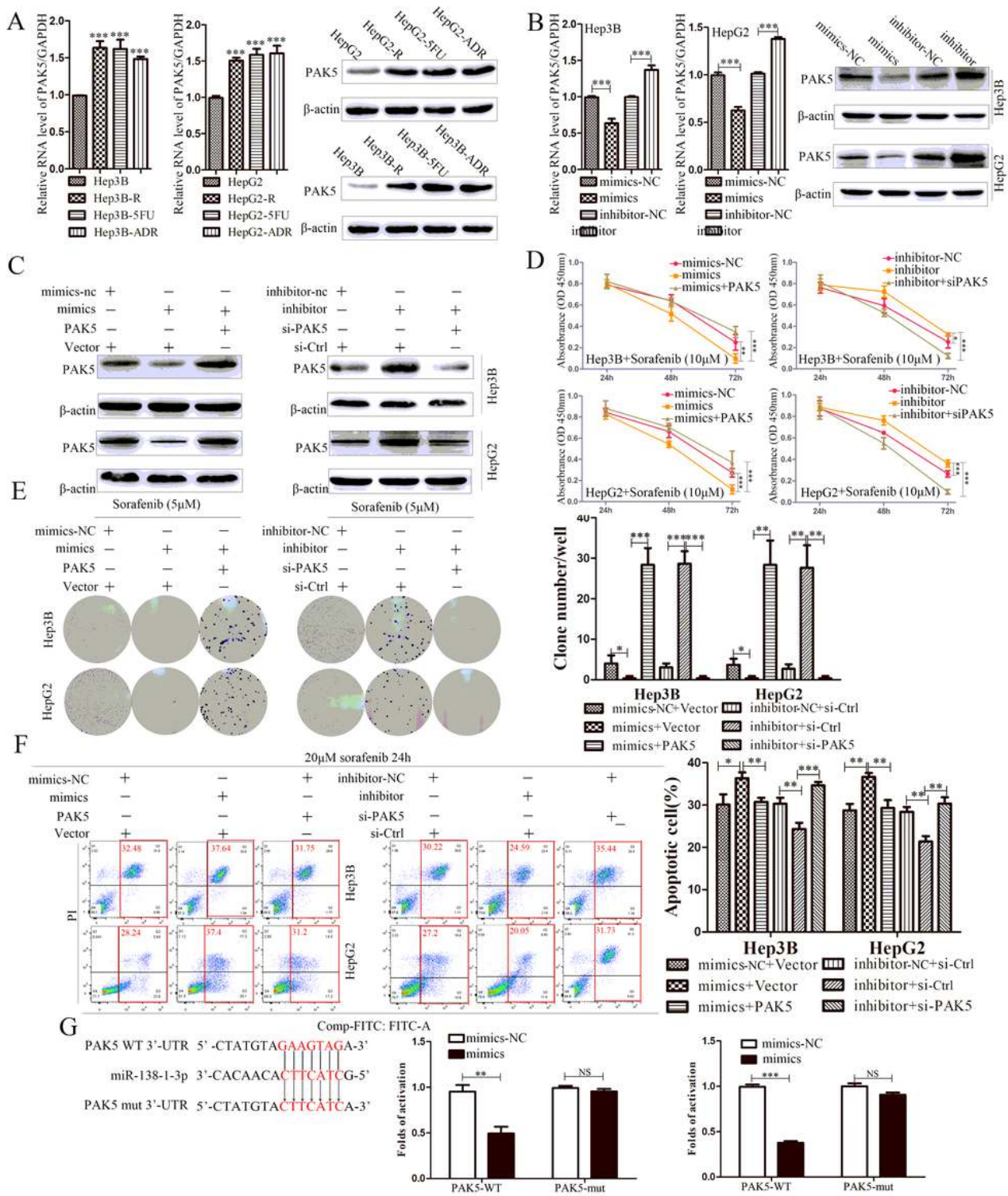

Figure 1

MiR-138-1-3p potentiated sensitivity of sorafenib to HCC. (A) CCK-8 assays in Hep3B, Hep3B-R and HepG2, HepG2-R cells after dealing with sorafenib at the concentration of 0, 10, 20, 30µM, 48hours. (B)

Representative images for plate colony formation assay in Hep3B, Hep3B-R and HepG2, HepG2-R cells after dealing with sorafenib at the concentration of 5μM, 10days. (C) Representative images for flow cytometric analysis of Hep3B, Hep3B-R and HepG2, HepG2-R cells after dealing with sorafenib at the concentration of 20μM, 24hours. (D) Relative miR-138-1-3p expression in HepG2, HepG2-ADR, HepG2-5FU, HepG2-R and HepG2, HepG2-ADR, HepG2-5FU, HepG2-R cells was detected by qRT-PCR, U6 was used as an internal control. (E) Conformation of the levels of miR-138-1-3p in transient transfected Hep3B and HepG2 cell lines by qRT-PCR, after transfected with miR-138-1-3p mimics or inhibitor with respective -NC control. (F) The cell viability was detected by CCK-8 assays after transfection of mimics or inhibitor with respective -NC control, dealing with sorafenib at the concentration of 10μM, 48hours. (G) Representative images for plate colony formation assay in Hep3B and HepG2 cells after transfection of mimics or inhibitor with respective -NC control and deal with sorafenib at the concentration of 5μM, 10days. (H) Representative images for flow cytometric analysis of HepG2 and Hep3B cell lines after transfection of mimics or inhibitor with respective -NC control and deal with sorafenib at the concentration of 20μM, 24hours.
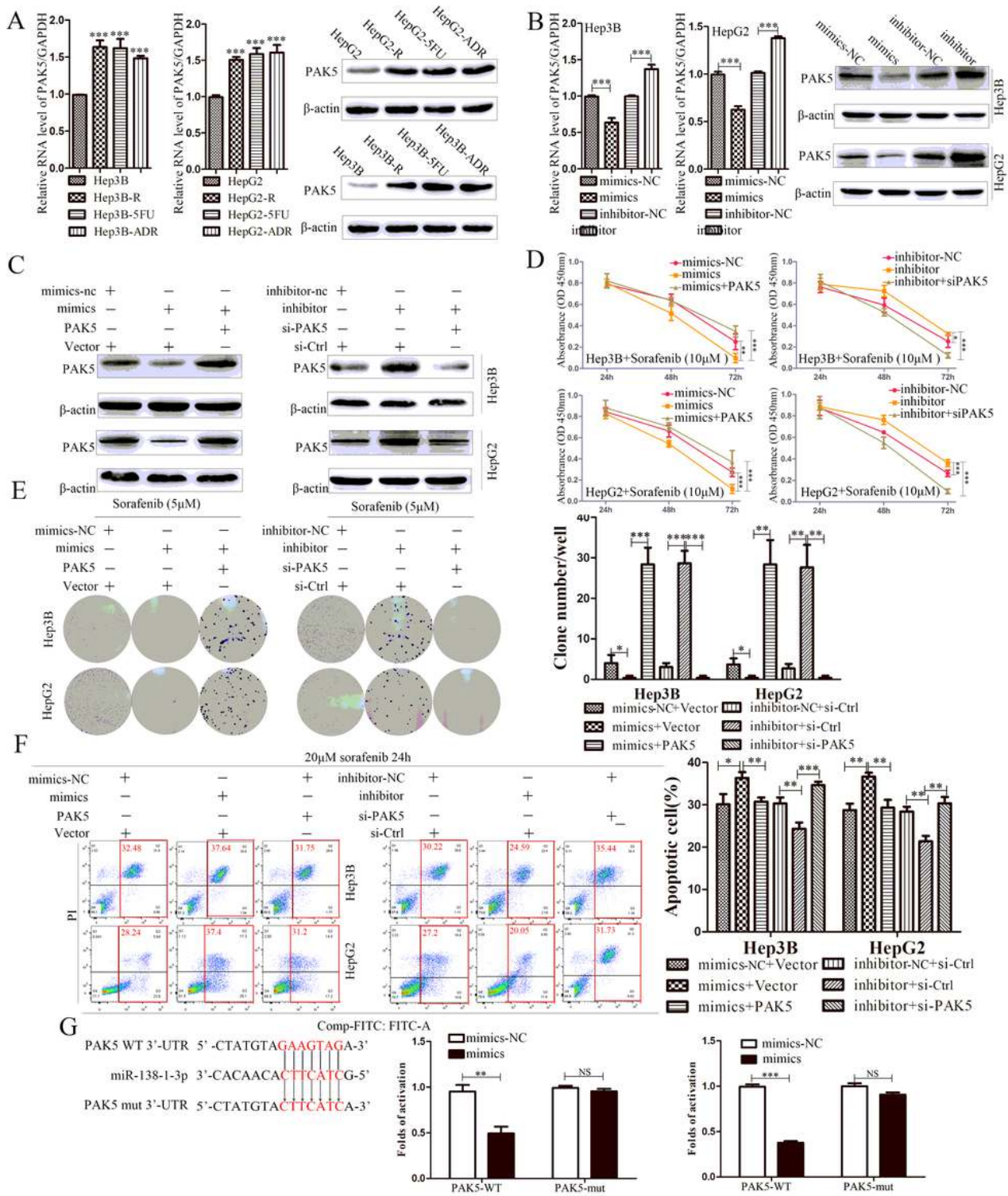
Figure 2

MiR-138-1-3p inhibited PAK5 expression by directly targeted the 3'-UTR of PAK5. (A) Relative PAK5 mRNA expression in HepG2, HepG2-ADR, HepG2-5FU, HepG2-R and HepG2, HepG2-ADR, HepG2-5FU, HepG2-R cells was detected by qRT-PCR, GAPDH was used as an internal control. Relative PAK5 protein expression in HepG2, HepG2-ADR, HepG2-5FU, HepG2-R and HepG2, HepG2-ADR, HepG2-5FU, HepG2-R cells was detected by Western Blot, β-actin was used as an internal control. (B) Relative PAK5 mRNA expression in

Hep3B and HepG2 after transfection of mimics or inhibitor with respective -NC control was detected by qRT-PCR, GAPDH was used as an internal control. (C) Relative PAK5 protein expression in Hep3B and HepG2 after co-transfection as shown was detected by Western Blot, β-actin was used as an internal control. (D) The cell viability was detected by CCK-8 assays after co-transfection as shown in Hep3B and HepG2 cells. (E) Representative images for plate colony formation assay after six groups of co-transfection as shown in Hep3B and HepG2 cells. (F) Representative images for flow cytometric analysis after six groups of co-transfection as shown in Hep3B and HepG2 cells. (G) Schematic description of wild type (WT) and mutated (mut) 3'-UTR of the PAK5 mRNA. Hep3B and HepG2 cells were co-transfected with mimics-NC or mimics and PAK5 WT 3'-UTR or PAK5 mut 3'-UTR for 48 hours and then dual luciferase reporter assay was employed to detect the reporter activity.
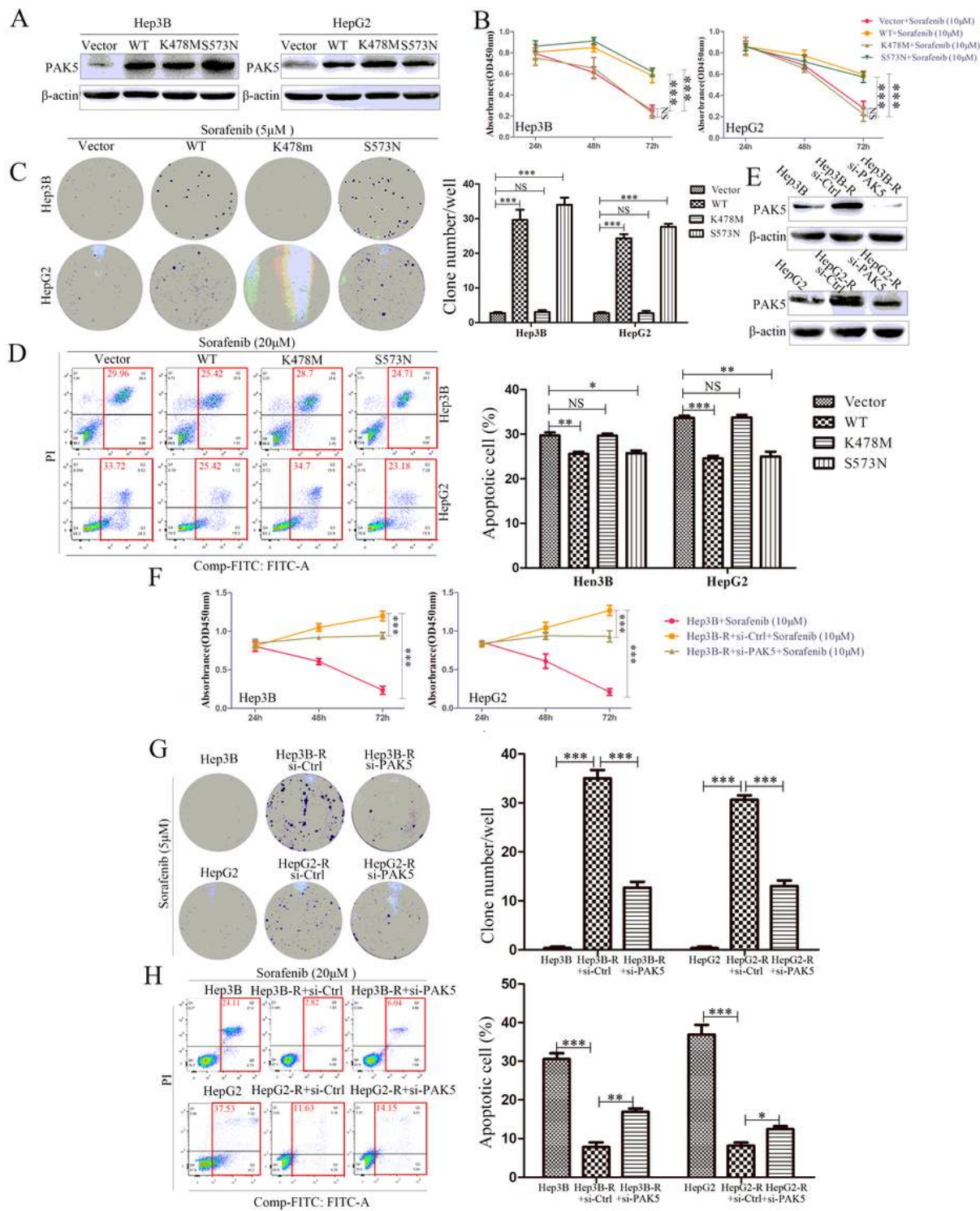
Figure 2

MiR-138-1-3p inhibited PAK5 expression by directly targeted the 3'-UTR of PAK5. (A) Relative PAK5 mRNA expression in HepG2, HepG2-ADR, HepG2-5FU, HepG2-R and HepG2, HepG2-ADR, HepG2-5FU, HepG2-R cells was detected by qRT-PCR, GAPDH was used as an internal control. Relative PAK5 protein expression in HepG2, HepG2-ADR, HepG2-5FU, HepG2-R and HepG2, HepG2-ADR, HepG2-5FU, HepG2-R cells was detected by Western Blot, β-actin was used as an internal control. (B) Relative PAK5 mRNA expression in

Hep3B and HepG2 after transfection of mimics or inhibitor with respective -NC control was detected by qRT-PCR, GAPDH was used as an internal control. (C) Relative PAK5 protein expression in Hep3B and HepG2 after co-transfection as shown was detected by Western Blot, β-actin was used as an internal control. (D) The cell viability was detected by CCK-8 assays after co-transfection as shown in Hep3B and HepG2 cells. (E) Representative images for plate colony formation assay after six groups of co-transfection as shown in Hep3B and HepG2 cells. (F) Representative images for flow cytometric analysis after six groups of co-transfection as shown in Hep3B and HepG2 cells. (G) Schematic description of wild type (WT) and mutated (mut) 3'-UTR of the PAK5 mRNA. Hep3B and HepG2 cells were co-transfected with mimics-NC or mimics and PAK5 WT 3'-UTR or PAK5 mut 3'-UTR for 48 hours and then dual luciferase reporter assay was employed to detect the reporter activity.
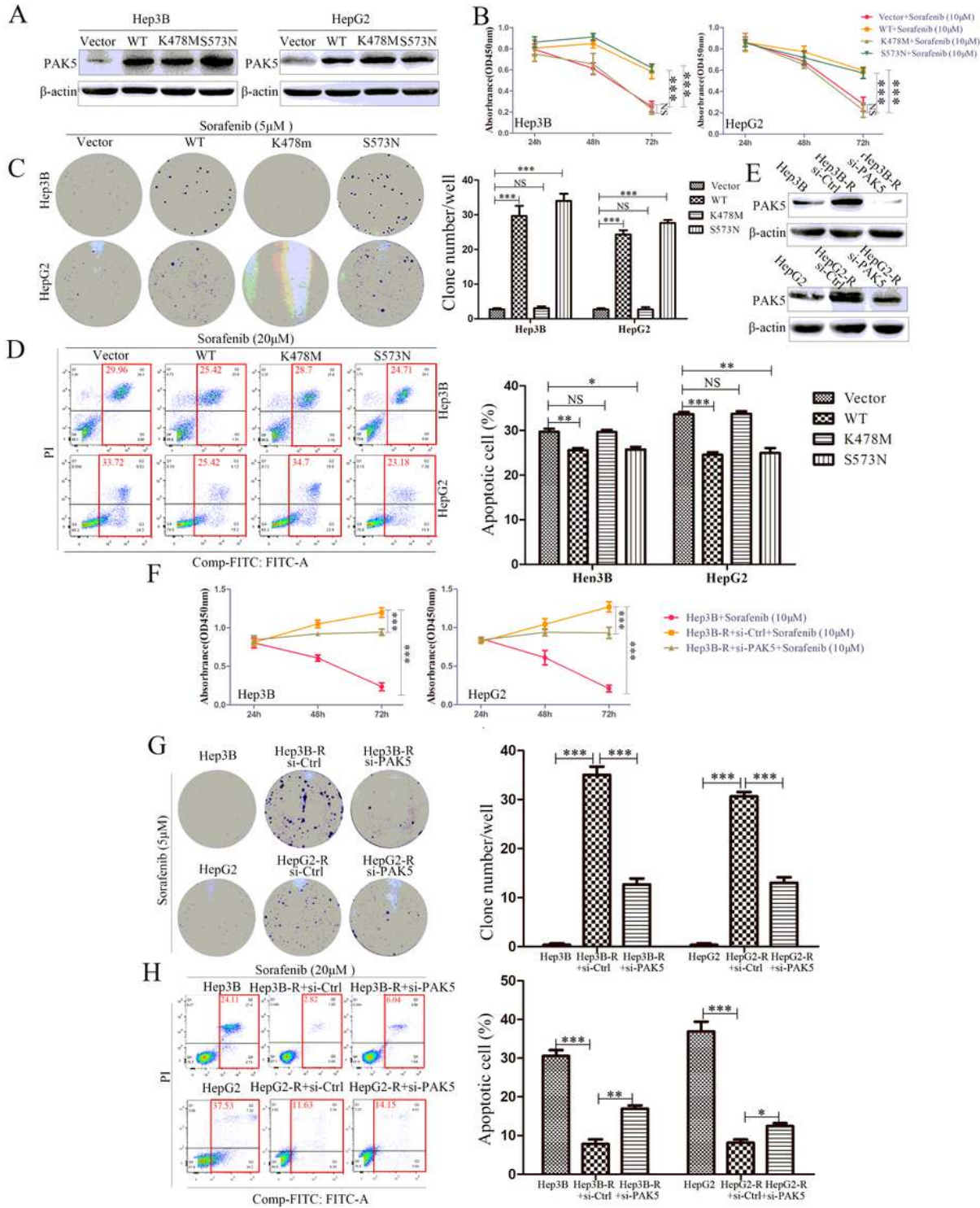
Figure 3

PAK5 eliminated the sorafenib induced cell apoptosis in HCC in vitro. (A) Conformation of the expression of PAK5 protein in four groups after transfection PAK5/PAK5/Vector, PAK5/WT, PAK5/K478M and PAK5/S573N as shown, β-actin was used as an internal control in Hep3B and HepG2 cells. (B) The cell viability was detected by CCK-8 assays after four groups of transfection (PAK5/Vector, PAK5/WT, PAK5/K478M and PAK5/S573N) in Hep3B and HepG2 cells. (C) Representative images for plate colony

formation assay after four groups of transfection (PAK5/Vector, PAK5/WT, PAK5/K478M and PAK5/S573N) in Hep3B and HepG2 cells. (D) Representative images for flow cytometric analysis after four groups of transfection (PAK5/Vector, PAK5/WT, PAK5/K478M and PAK5/S573N) in Hep3B and HepG2 cells. (E) Conformation of the expression of PAK5 protein in three groups as shown. (F) The cell viability was detected by CCK-8 assays after three groups as shown. (G) Representative images for plate colony formation assay after three groups as shown. (H) Representative images for flow cytometric analysis after three groups as shown. NS represented statistical difference.
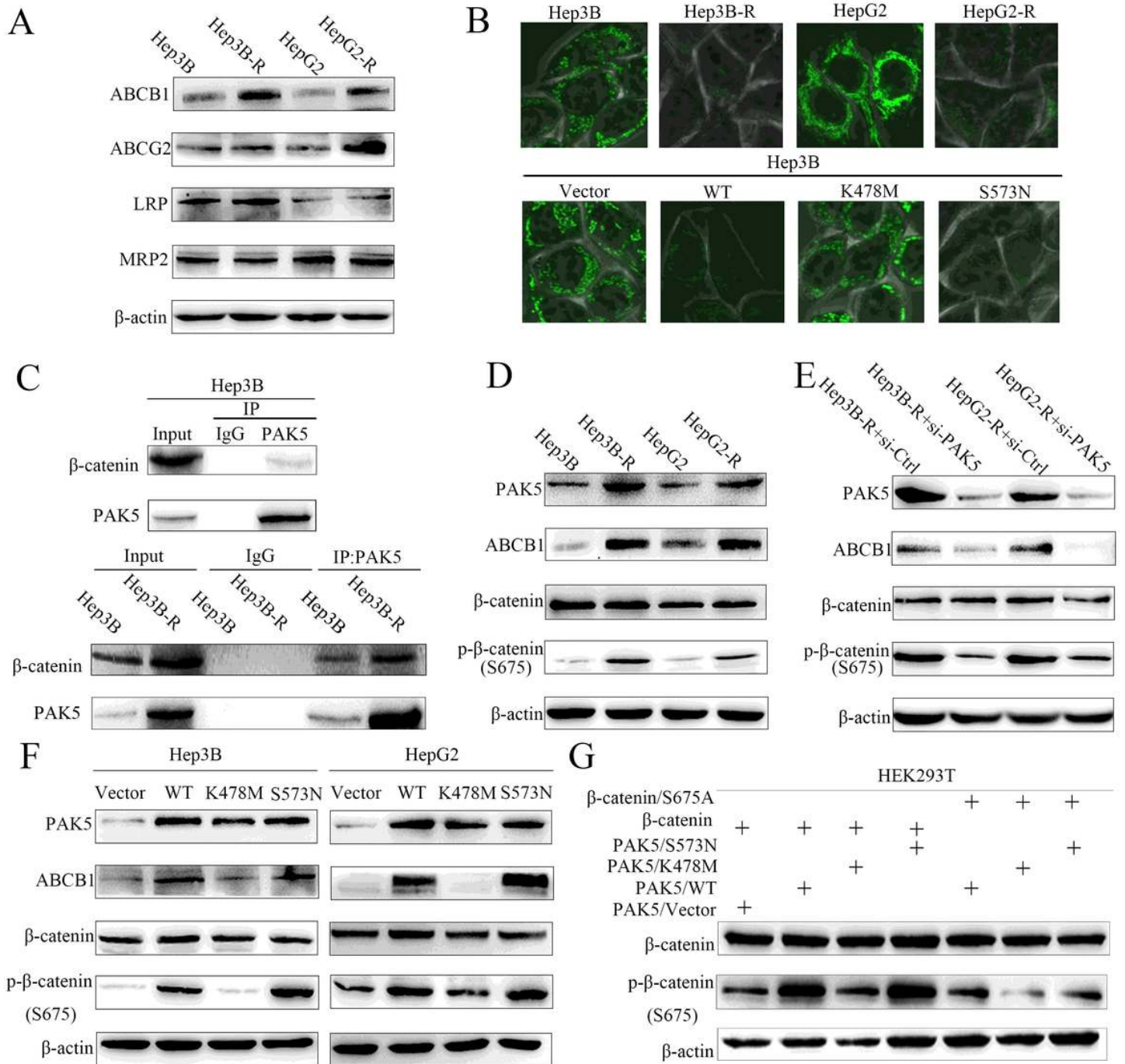
Figure 3

PAK5 eliminated the sorafenib induced cell apoptosis in HCC in vitro. (A) Conformation of the expression of PAK5 protein in four groups after transfection PAK5/PAK5/Vector, PAK5/WT, PAK5/K478M and PAK5/S573N as shown, β-actin was used as an internal control in Hep3B and HepG2 cells. (B) The cell viability was detected by CCK-8 assays after four groups of transfection (PAK5/Vector, PAK5/WT, PAK5/K478M and PAK5/S573N) in Hep3B and HepG2 cells. (C) Representative images for plate colony formation assay after four groups of transfection (PAK5/Vector, PAK5/WT, PAK5/K478M and PAK5/S573N) in Hep3B and HepG2 cells. (D) Representative images for flow cytometric analysis after four groups of transfection (PAK5/Vector, PAK5/WT, PAK5/K478M and PAK5/S573N) in Hep3B and HepG2 cells. (E) Conformation of the expression of PAK5 protein in three groups as shown. (F) The cell viability was detected by CCK-8 assays after three groups as shown. (G) Representative images for plate colony formation assay after three groups as shown. (H) Representative images for flow cytometric analysis after three groups as shown. NS represented statistical difference.

Figure 4

PAK5 promoted ABCB1 transcriptional activation via Wnt/β-catenin signaling pathway. (A) Relative multidrug resistance proteins (ABCB1, ABCG2, LRP and MRP2) expression in Hep3B, Hep3B-R and HepG2, HepG2-R cells was detected by Western Blot, β-actin was used as an internal control. (B) The fluorescent dye rhodamine 123 (Rho123) as an index for P-gp activity in Hep3B, Hep3B-R and HepG2, HepG2-R cells. The fluorescent dye rhodamine 123 (Rho123) was detected after four groups of transfection (PAK5/Vector, PAK5/WT, PAK5/K478M and PAK5/S573N) in Hep3B cells. (C) Hep3B cells were immunoprecipitated with anti-PAK5 antibody and immunoblotted with anti-PAK5 and anti-β-catenin

antibody. Hep3B and Hep3B-R cells were immunoprecipitated with anti-PAK5 antibody and immunoblotted with anti-PAK5 and anti-β-catenin antibody. (D) Relative proteins (PAK5, ABCB1, β-catenin, p-β-catenin (S675)) expression in Hep3B, Hep3B-R and HepG2, HepG2-R cells was detected by Western Blot, β-actin was used as an internal control. (E) Relative proteins (PAK5, ABCB1, β-catenin, p-β-catenin (S675)) expression in Hep3B and HepG2 cells after transient transfection PAK5/Vector, PAK5/WT, PAK5/K478M and PAK5/S573N plasmids respectively was detected by Western Blot, β-actin was used as an internal control. (F) Relative proteins (PAK5, ABCB1, β-catenin, p-β-catenin (S675)) expression after transient transfection siPAK5 and their negative control in Hep3B and HepG2 cells was detected by Western Blot, β-actin was used as an internal control. (G) β-catenin and p-β-catenin (S675) proteins expression after seven groups of co-transfection as shown in HEK293T cells was detected by Western Blot, β-actin was used as an internal control.
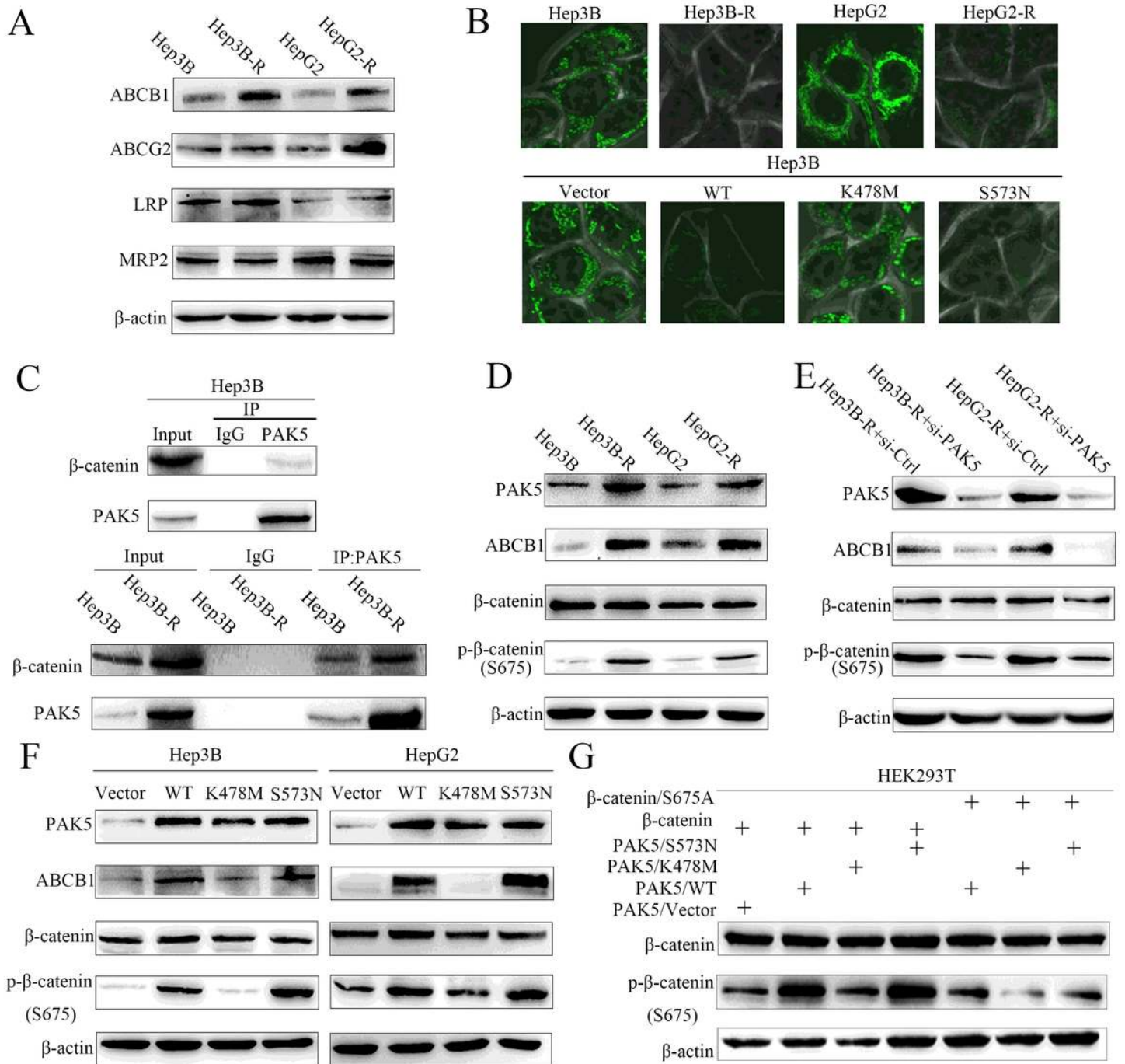
Figure 4

PAK5 promoted ABCB1 transcriptional activation via Wnt/β-catenin signaling pathway. (A) Relative multidrug resistance proteins (ABCB1, ABCG2, LRP and MRP2) expression in Hep3B, Hep3B-R and HepG2, HepG2-R cells was detected by Western Blot, β-actin was used as an internal control. (B) The fluorescent dye rhodamine 123 (Rho123) as an index for P-gp activity in Hep3B, Hep3B-R and HepG2, HepG2-R cells. The fluorescent dye rhodamine 123 (Rho123) was detected after four groups of transfection (PAK5/Vector, PAK5/WT, PAK5/K478M and PAK5/S573N) in Hep3B cells. (C) Hep3B cells were immunoprecipitated with anti-PAK5 antibody and immunoblotted with anti-PAK5 and anti-β-catenin

antibody. Hep3B and Hep3B-R cells were immunoprecipitated with anti-PAK5 antibody and immunoblotted with anti-PAK5 and anti-β-catenin antibody. (D) Relative proteins (PAK5, ABCB1, β-catenin, p-β-catenin (S675)) expression in Hep3B, Hep3B-R and HepG2, HepG2-R cells was detected by Western Blot, β-actin was used as an internal control. (E) Relative proteins (PAK5, ABCB1, β-catenin, p-β-catenin (S675)) expression in Hep3B and HepG2 cells after transient transfection PAK5/Vector, PAK5/WT, PAK5/K478M and PAK5/S573N plasmids respectively was detected by Western Blot, β-actin was used as an internal control. (F) Relative proteins (PAK5, ABCB1, β-catenin, p-β-catenin (S675)) expression after transient transfection siPAK5 and their negative control in Hep3B and HepG2 cells was detected by Western Blot, β-actin was used as an internal control. (G) β-catenin and p-β-catenin (S675) proteins expression after seven groups of co-transfection as shown in HEK293T cells was detected by Western Blot, β-actin was used as an internal control.

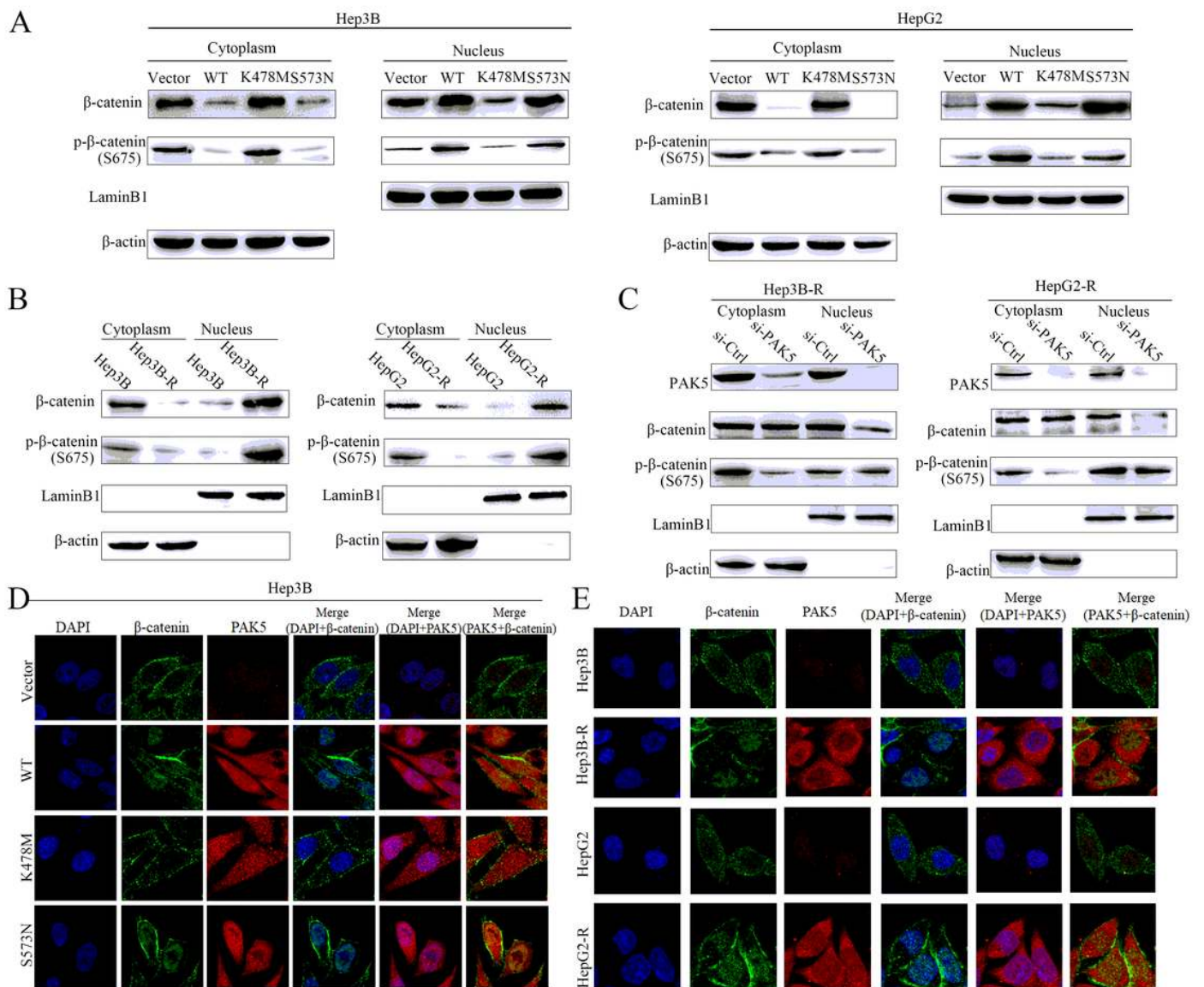Figure 5

PAK5 facilitated the nuclear translocation of β-catenin. (A) The nuclear and cytoplasmic fractionation was employed to test the cellular distribution of β-catenin and p-β-catenin (S675) in Hep3B and HepG2 cells after transfecting PAK5/Vector, PAK5/WT, PAK5/S573N and PAK5/K478M respectively. β-actin and LaminB1 was used as an internal control. (B) The nuclear and cytoplasmic fractionation was employed to test the cellular distribution of β-catenin and p-β-catenin (S675) in Hep3B, Hep3B-R and HepG2, HepG2-R cells. β-actin and LaminB1 was used as an internal control. (C) The nuclear and cytoplasmic fractionation was employed to test the cellular distribution of β-catenin and p-β-catenin (S675) after transient transfection siPAK5 and their negative control in Hep3B-R and HepG2-R cells. β-actin and LaminB1 was used as an internal control. (D) and (E) Representative images of immunofluorescence staining followed four groups of transfection (PAK5/Vector, PAK5/WT, PAK5/K478M and PAK5/S573N) in Hep3B and HepG2 cells (left). Representative images of immunofluorescence staining of Hep3B, Hep3B-R and HepG2, HepG2-R cells (right). The positive signal (red) represented PAK5, the positive signal (green) represented β-catenin, and the positive signal (blue) represented DAPI.
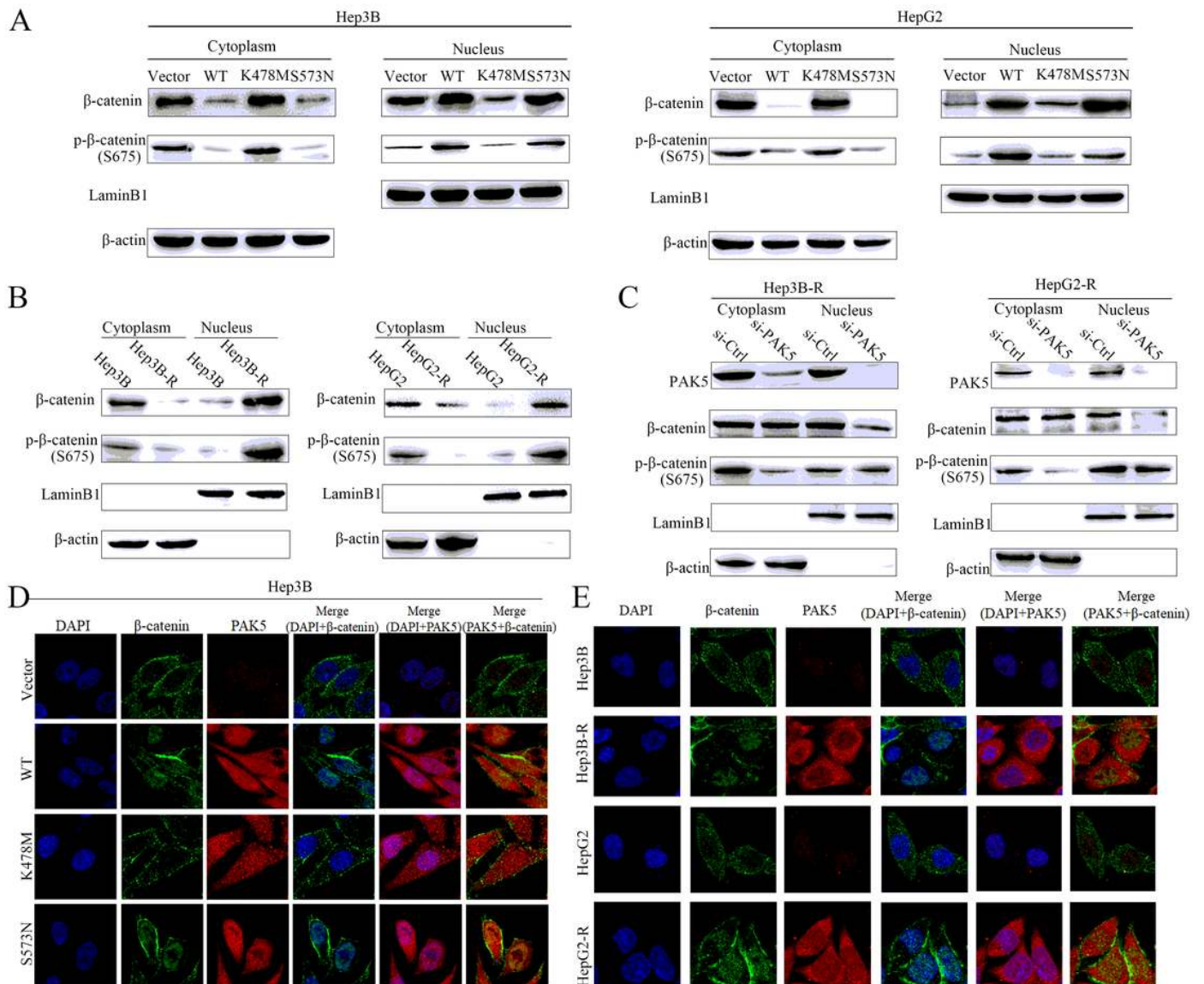
Figure 5

PAK5 facilitated the nuclear translocation of β-catenin. (A) The nuclear and cytoplasmic fractionation was employed to test the cellular distribution of β-catenin and p-β-catenin (S675) in Hep3B and HepG2 cells after transfecting PAK5/Vector, PAK5/WT, PAK5/S573N and PAK5/K478M respectively. β-actin and LaminB1 was used as an internal control. (B) The nuclear and cytoplasmic fractionation was employed to test the cellular distribution of β-catenin and p-β-catenin (S675) in Hep3B, Hep3B-R and HepG2, HepG2-R cells. β-actin and LaminB1 was used as an internal control. (C) The nuclear and cytoplasmic fractionation was employed to test the cellular distribution of β-catenin and p-β-catenin (S675) after transient transfection siPAK5 and their negative control in Hep3B-R and HepG2-R cells. β-actin and LaminB1 was used as an internal control. (D) and (E) Representative images of immunofluorescence staining followed four groups of transfection (PAK5/Vector, PAK5/WT, PAK5/K478M and PAK5/S573N) in Hep3B and HepG2 cells (left). Representative images of immunofluorescence staining of Hep3B, Hep3B-R and HepG2, HepG2-R cells (right). The positive signal (red) represented PAK5, the positive signal (green) represented β-catenin, and the positive signal (blue) represented DAPI.
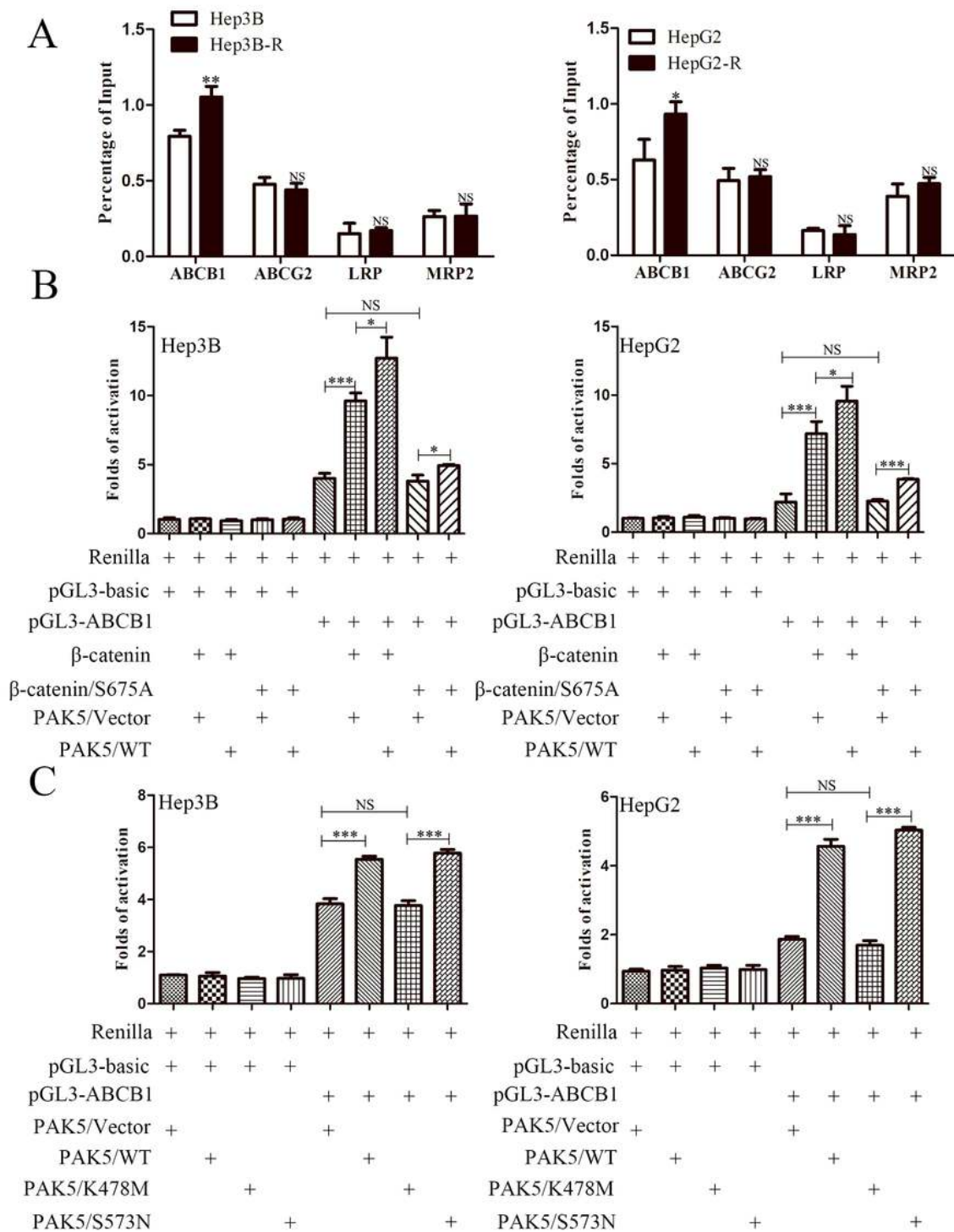
Figure 6

β-catenin targeted ABCB1 promoter and active. (A) CHIP with β-catenin antibody in Hep3B and HepG2 cells treated with ABCB1, ABCG2, LRP and MRP2 were employed to scrutinize the target genes. Detected by qRT-PCR, GAPDH was used as an internal control. (B) and (C) Dual luciferase reporter assay was used to detect the reporter activity after ten or twelve groups' co-transfected as shown in Hep3B and HepG2 cells.
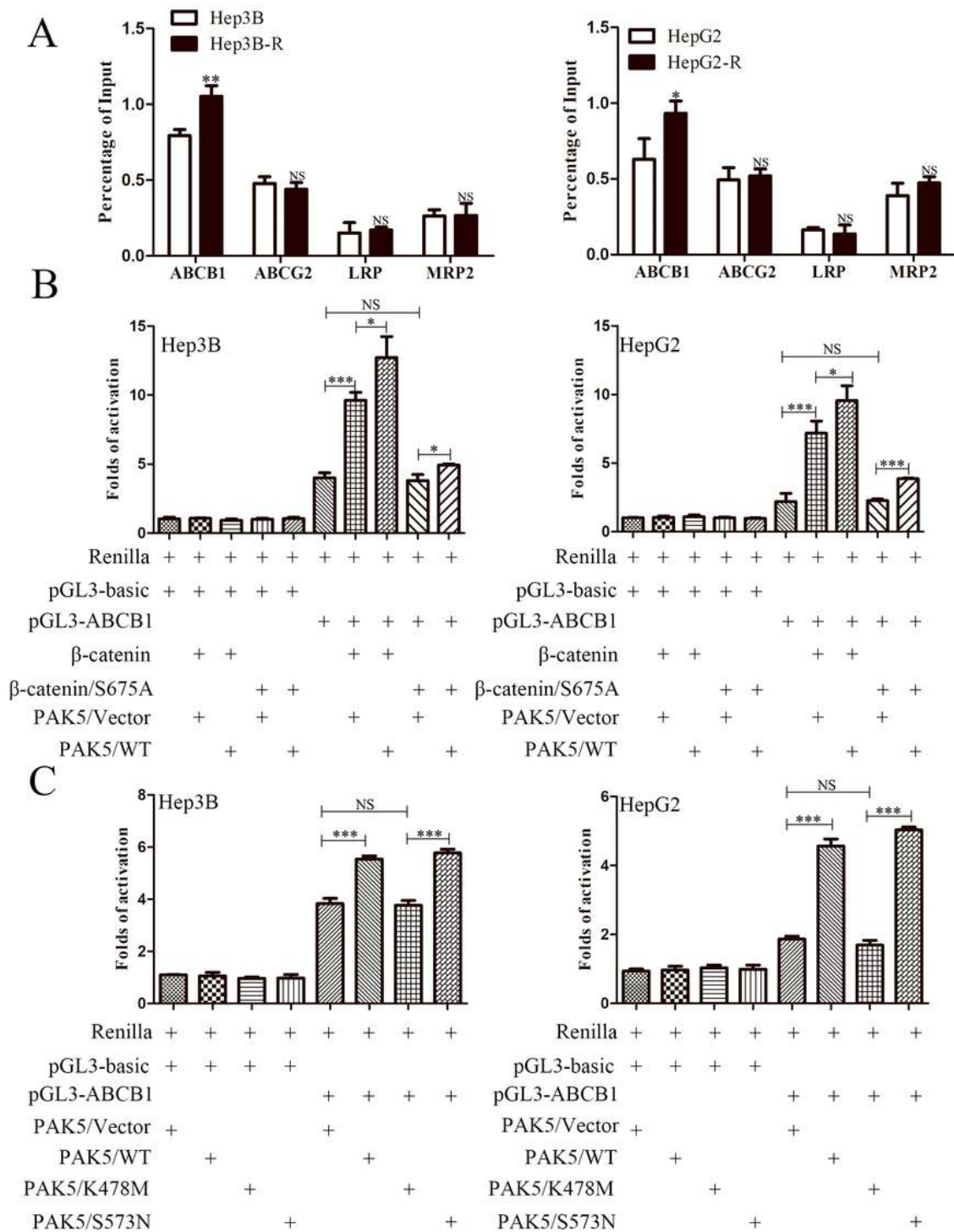
Figure 6

β-catenin targeted ABCB1 promoter and active. (A) CHIP with β-catenin antibody in Hep3B and HepG2 cells treated with ABCB1, ABCG2, LRP and MRP2 were employed to scrutinize the target genes. Detected by qRT-PCR, GAPDH was used as an internal control. (B) and (C) Dual luciferase reporter assay was used to detect the reporter activity after ten or twelve groups' co-transfected as shown in Hep3B and HepG2 cells.
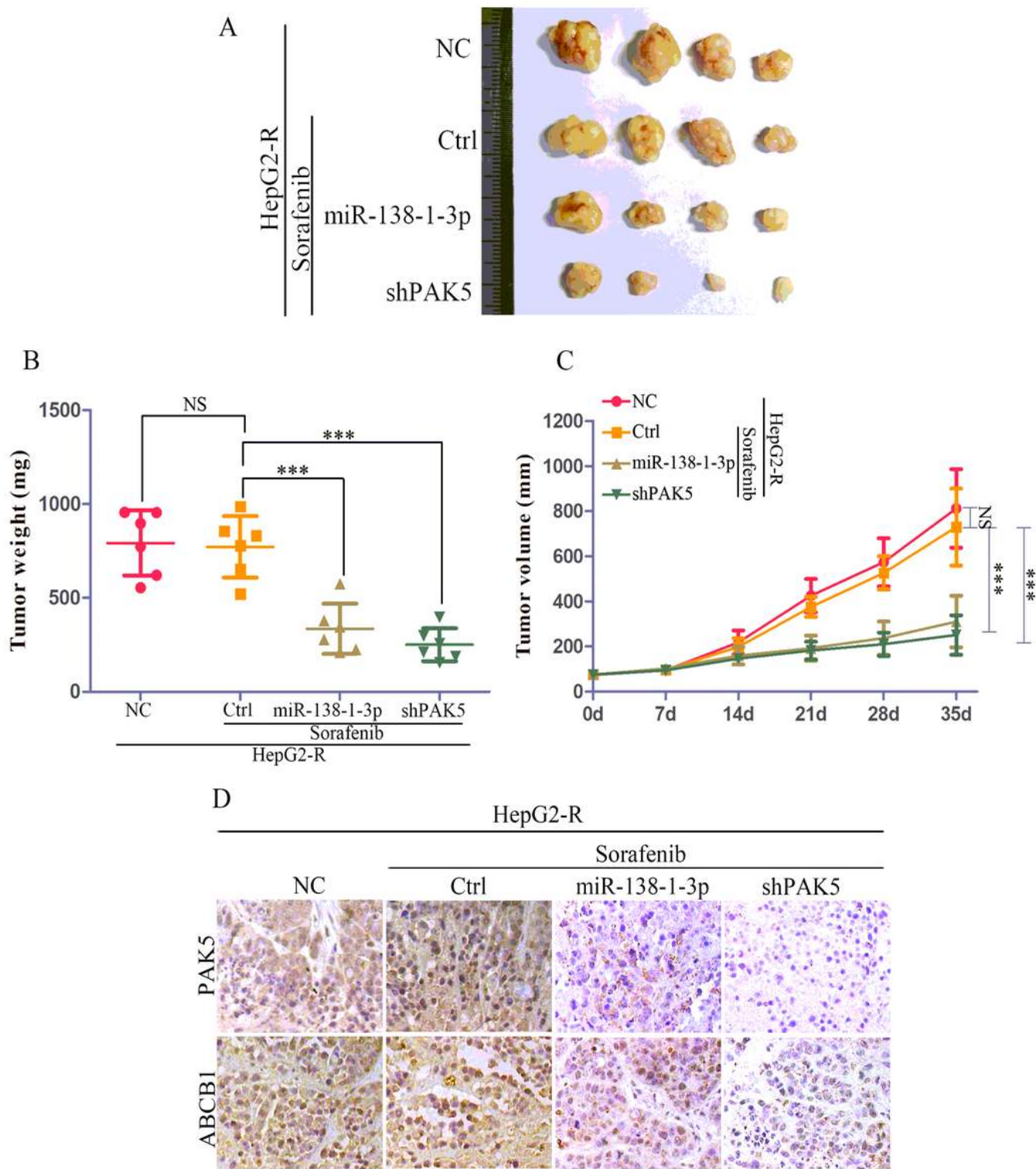
Figure 7

MiR-138-1-3p sensitized sorafenib to HCC by targeting PAK5 in vivo. (A) Xenograft tumor formation of HepG2-R cells in nude mice. (B) (D) The weight and volume of tumor cancer models were analyzed and calculated as shown. (E) Representative images of PAK5 and ABCB1 immunohistochemical staining with PAK5 and ABCB1 antibodise in four groups as shown.
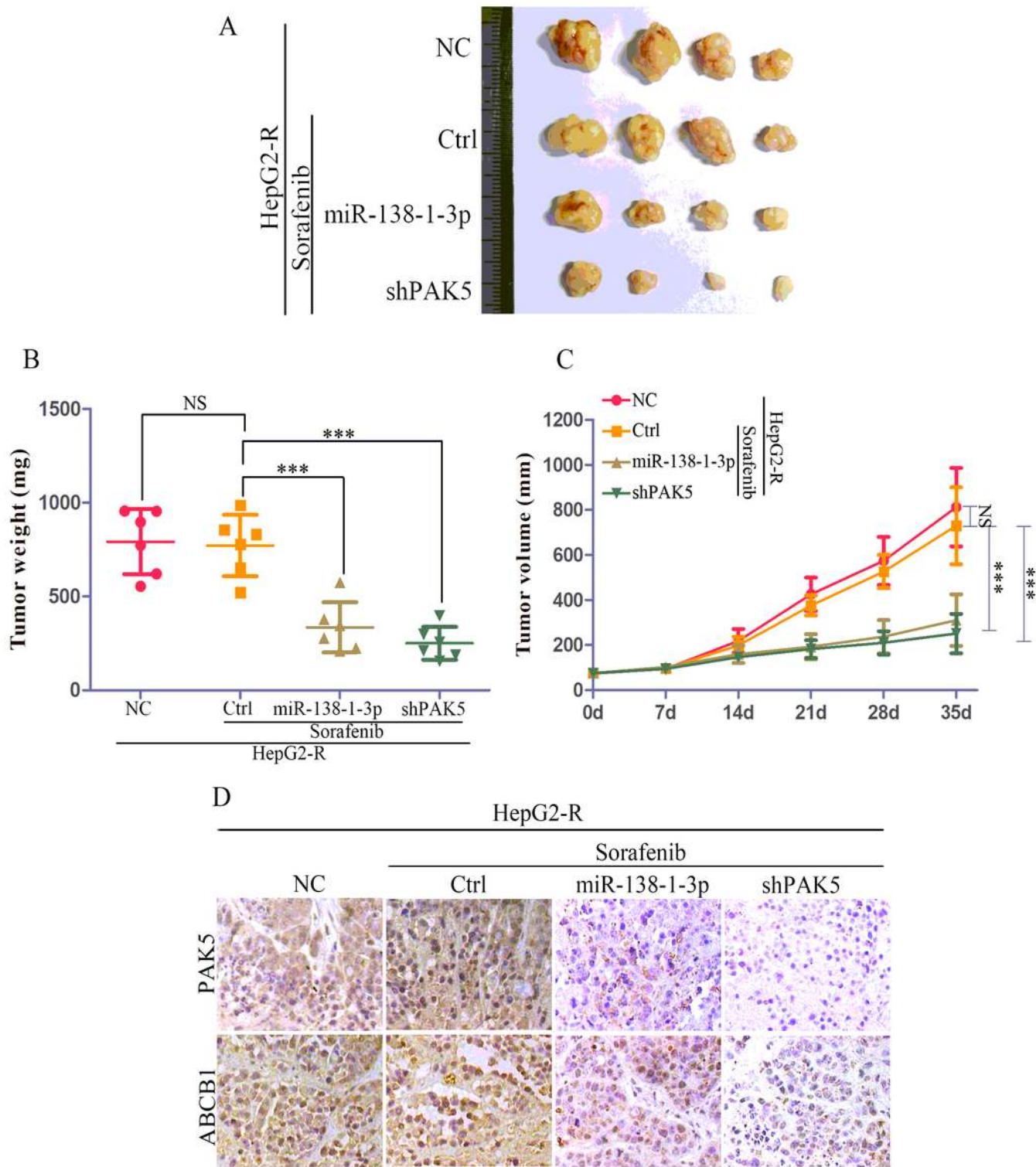
Figure 7

MiR-138-1-3p sensitized sorafenib to HCC by targeting PAK5 in vivo. (A) Xenograft tumor formation of HepG2-R cells in nude mice. (B) (D) The weight and volume of tumor cancer models were analyzed and calculated as shown. (E) Representative images of PAK5 and ABCB1 immunohistochemical staining with PAK5 and ABCB1 antibodise in four groups as shown.